PHYSICAL REVIEW D **82,** 015007 (2010)

Distinguishing dark matter stabilization symmetries using multiple kinematic edges and cusps

Kaustubh Agashe,[1] Doojin Kim,[1] Manuel Toharia,[1] and Devin G. E. Walker[2,3,4]

[1]*Maryland Center for Fundamental Physics, Department of Physics, University of Maryland, College Park, Maryland 20742, USA*
[2]*Department of Physics, University of California, Berkeley, California 94720, USA*
[3]*Theoretical Physics Group, Lawrence Berkeley National Laboratory, Berkeley, California 94720, USA*
[4]*Center for the Fundamental Laws of Nature, Jefferson Physical Laboratory, Harvard University, Cambridge, Massachusetts 02138, USA*

(Received 20 April 2010; published 19 July 2010)

We emphasize that the stabilizing symmetry for dark matter (DM) particles does not have to be the commonly used parity (Z_2) symmetry. We therefore examine the potential of the colliders to distinguish models with parity stabilized DM from models in which the DM is stabilized by other symmetries. We often take the latter to be a Z_3 symmetry for illustration. We focus on signatures where a *single* particle, charged under the DM stabilization symmetry decays into the DM and standard model (SM) particles. Such a Z_3-charged mother particle can decay into *one or two* DM particles along with the *same* SM particles. This can be contrasted with the decay of a Z_2-charged mother particle, where only one DM particle appears. Thus, if the intermediate particles in these decay chains are *off*-shell, then the reconstructed invariant mass of the SM particles exhibits two kinematic edges for the Z_3 case but only one for the Z_2 case. For the case of *on*-shell intermediate particles, distinguishing the two symmetries requires more than the kinematic edges. In this case, we note that certain decay chain topologies of the mother particle which are present for the Z_3 case (but absent for the Z_2 case) generate a cusp in the invariant mass distribution of the SM particles. We demonstrate that this cusp is generally invariant of the various spin configurations. We further apply these techniques within the context of explicit models.

DOI: 10.1103/PhysRevD.82.015007 PACS numbers: 14.80.−j

I. INTRODUCTION

There is compelling evidence for the existence of dark matter (DM) in the universe [1]. These observations can be explained by the postulating of new stable particles. A consensus picture of the nature of such a particle is provided by a host of astrophysical, cosmological, and direct detection experiments: A viable DM candidate must be electrically neutral and colorless, nonrelativistic at redshifts of $z \sim 3000$ and generate the measured relic abundance of $h^2\Omega_{\rm DM} = 0.1131 \pm 0.0034$ [2]. Additionally a weakly interacting massive particle (WIMP) is a very well-motivated paradigm [1]. Consider DM particles as relics which were once in thermal equilibrium with the rest of the universe. It is well known that the measured relic abundance is correlated with the dark matter annihilation cross section [3] by

$$h^2\Omega_{\rm DM} \simeq \frac{0.1\ \text{pb}\cdot c}{\langle\sigma v\rangle}. \tag{1}$$

The annihilation cross section of a pair of dark matter particles into a two particle final state goes as

$$\langle\sigma v\rangle \sim \frac{g^4}{8\pi}\frac{1}{M^2}, \tag{2}$$

where g denotes the couplings and M the masses of the particles in the dark sector. This cross section is naturally of the right value for $g \sim \mathcal{O}(1)$ and $M \sim 100$ GeV. Moreover, many extensions of the standard model (SM) at the weak scale, most of which are invoked primarily as solutions to other problems of the SM (most notably the Planck-weak hierarchy problem), contain such stable WIMPs. Because of this possibility, it may be possible to detect DM directly via scattering off nuclei or indirectly via detection of its (SM) annihilation products [1].

Such a scenario also makes the idea of dark matter amenable for testing at the high-energy colliders. It is possible to produce only DM particles directly at colliders, but then we do not have any visible signal since the DM particles will simply escape these detectors without interacting. Instead we investigate events where the dark matter is produced (indirectly) along with visible SM particles from the decays of particles charged under both dark matter stabilization (but heavier than the DM) and the unbroken SM symmetries. The existence of such mother particles is a feature of almost all models of physics beyond the SM that contain stable WIMPs.

To date, a tremendous amount of effort has been made to reconstruct such events at the upcoming Large Hadron Collider (LHC) in order to determine the masses of the DM, the mother particles and possibly intermediate particles in the decay chains. For example, see Refs. [4–7]. Most of this work has been for parity (Z_2) stabilized dark matter. This is because the most popular models, e.g. supersymmetric (SUSY), little Higgs, and extra-dimensional scenarios [8–12], all ensure the dark matter candidates remain stable by employing a Z_2 stabilization symmetry. Importantly these models have served as a guide of expected signatures of dark matter at the LHC [13,14].

In this paper we emphasize that any discrete or continuous global symmetry can be used to stabilize dark matter.[1] Furthermore, because all fundamental particles in nature are defined by how they transform under various symmetries, most of the popular (Z_2) models actually consider only one type of DM candidate. It is therefore critical to determine *experimentally*, i.e., without theoretical bias, the nature of the symmetry that stabilizes dark matter. We embark on a program of study to distinguish models in which the DM is stabilized by a Z_2 discrete symmetry from models in which the DM is stabilized with other symmetries. A beginning effort was made in Ref. [16] which focused on signatures with long-lived mother particles, i.e., which decay to DM and the SM particles *outside* of the detector. In this paper we study the complementary possibility of mother particles which decay to DM and the SM particles *inside* of the detector.

Our main idea is that the final states and the ''topology'' of the decay of a mother particle are (in part) determined by the DM stabilization symmetry. Thus reconstructing the visible parts of these decay chains will allow us to differentiate a model of DM stabilized with a non-Z_2 symmetry from one where DM is stabilized with a Z_2 symmetry. In this paper we begin to explore such signatures. Our conclusions seem generic for most stabilization symmetries that are not parity symmetries; however, for definiteness, we focus on the case of a Z_3 symmetry. When illustrating the signatures we will generically refer to any model stabilized with Z_2 and Z_3 stabilization symmetry simply as Z_2 and Z_3 models, respectively.

More specifically to see differences between Z_2 and Z_3 models, we focus on the *kinematic edges* and *shapes* of invariant mass distributions of the SM particles resulting from the decay of a *single* mother particle charged under the SM and the DM stabilization symmetries. We note the possibility of one or two DM particles in each decay chain being allowed by the Z_3 symmetry (along with SM particles which can, in general, be different in the two decay chains). Whereas, in Z_2 models, decays of a mother particle in given SM final state cannot have two DM particles in the decay chain and hence typically has only one DM particle. Thus,

(i) If all the intermediate particles in the two decay chains are *off-shell* and the SM particles in the two decay chains are the *same*, then we show that there are two Z_3 kinematic edges in the invariant mass distribution of this SM final state at approximately $M_{\text{mother}} - m_{\text{DM}}$ and $M_{\text{mother}} - 2m_{\text{DM}}$. Models with Z_2 stabilized dark matter have only one endpoint approximately given by $M_{\text{mother}} - m_{\text{DM}}$.

[1] Gauge symmetries alone cannot be used to stabilize dark matter. See the discussion in Ref. [15].

In the case of on-shell intermediate particles, the decay of such a mother in a Z_3 model can similarly result in double edges due to the presence of one or two DM in the final state. However, in this case the endpoint also depends on the masses of intermediate particles. Thus it is possible to obtain multiple edges even from decay of a single mother particle in a Z_2 model due to different intermediate particles to the same final state. Hence, multiple edges are not a robust way to distinguish between Z_3 and Z_2 symmetries in the case of on-shell intermediate particles. For the case of on-shell intermediate particles, we thus use shapes of invariant mass distributions instead of edges. In particular,

(i) We find a unique decay chain topology with two SM particles separated by a DM particle (along with another DM at the end of the decay chain) which is generally present for Z_3 models but absent for the Z_2 case. Based on pure kinematics/phase space, this topology leads to a cusp (i.e., derivative discontinuity) in the invariant mass distribution of the SM particles.

Of course for a generic model, it is possible to have a ''hybrid'' scenario where elements from the *on-shell* and *off-shell* scenarios are present.

An outline of the paper is as follows: In the next section, we begin with the case of off-shell intermediate particles in a decay chain. There we show how differing kinematic edges can be used to distinguish Z_2 from Z_3 models. In Sec. III we move on to the case of intermediate particles being on-shell. There we show the existence of a cusp in Z_3 models for certain topologies; further we show that this cuspy feature survives even when taking spin correlations into consideration. We then discuss a couple of explicit models—one based on warped extra-dimensional framework [17,18] and another using DM stabilization symmetry from spontaneous breaking [15]; see also Ref. [19] for another example of a Z_3-model. Here DM is not stabilized by Z_2 symmetries. In the second model, we show our signal is invariant under basic detector and background cuts. We next conclude and briefly enumerate how Z_2 models can fake signals from Z_3 models. We also mention future work to better reconstruct and distinguish Z_3 from Z_2 models, e.g., using the *two* such decay chains present in each full event.

II. OFF-SHELL INTERMEDIATE PARTICLES

In this paper, we mostly study the decay of a *single* heavy particle, which is charged under the dark matter stabilization and SM symmetries, into SM and dark matter candidate(s) *inside* the detector. Henceforth, we denote such heavy particles by mother particles. In this section we assume that all intermediate particles (if any) in this decay chain are *off*-shell. This off-shell scenario has been frequently studied by the ATLAS and CMS collaborations

[13,14] for SUSY theories (which is an example of a Z_2 model).

We consider constructing the invariant mass distribution of the (visible) decay products. Unlike for the Z_2 case, for Z_3 models a mother particle A can decay into one or two DM particles along with (in general different) SM particles. We mostly assume, just for simplicity, that there exist two visible particles (a, b or c, d) in the final state as shown below (note however that the same argument is relevant to the general cases where more than two visible particles are emitted)[2]:

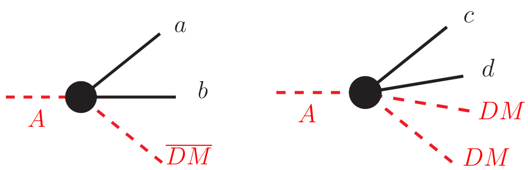

(3)

Here (and henceforth) the "blob" denotes intermediate particles in the decay which are off-shell. Also, uppercase letters/red/dashed lines denote particles charged under the DM symmetry (Z_3 or Z_2) and lowercase letters/black/solid lines denote SM (or "visible," as opposed to DM) particles, including, for example, a W boson. Such an unstable SM particle decays further into SM fermions, at least some of which are observed by the particle detector.

In order to avoid any possible confusion, we would like to explain the above diagrams. Under the Z_3 symmetry, a particle/field ϕ transforms as

$$\phi \rightarrow \phi \exp\left(\frac{2\pi i q}{3}\right), \tag{4}$$

where $q = 0$ (i.e., Z_3-neutral) or $q = 1,\ 2$ (nontrivial Z_3-charge). Suppose the lightest of the Z_3-charged particles (labeled ϕ_0) has charge $q = 1$ (similar argument goes through for charge $q = 2$ for ϕ_0). Clearly, its antiparticle ($\bar{\phi}_0$) has (a different) charge $q = -1$ (which is equivalent to $q = 2$) and has same mass as ϕ_0. Then, solely based on Z_3 symmetry considerations, all other (heavier) Z_3-charged particles can decay into this lightest Z_3-charged particle (in addition to Z_3-neutral particles, including SM ones). To be explicit, a heavier Z_3-charged particle with charge $q = 1$ can decay into either (single) ϕ_0 or *two* $\bar{\phi}_0$'s (and Z_3-neutral particles). Taking the *CP* conjugate of the preceding statement, we see that a heavier Z_3-charged particle with the other type of charge, namely $q = 2$, is allowed to decay into *two* ϕ_0's or single $\bar{\phi}_0$. Of course, ϕ_0 cannot decay and thus is the (single) DM candidate in this theory. We denote this DM particle and its antiparticle by DM and $\bar{\text{DM}}$, respectively, in above diagram (and henceforth), although we do not make this distinction in the text since DM and anti-DM particles are still degenerate.[3]

For simplicity, we assume that the SM (or visible) parts of the event can be completely reconstructed.[4] Considering the invariant masses m_{ab} and m_{cd}, which are formed by the two SM particles a, b and c, d in each decay chain, one can easily derive the minimum and the maximum kinematic endpoints of the distributions of m_{ab} and m_{cd} which are given by [20]:

$$m_{ab}^{\min} = m_a + m_b, \tag{5}$$

$$m_{ab}^{\max} = M_{\text{mother}} - m_{\text{DM}} \qquad \text{[Left process of Eq. (9)]}, \tag{6}$$

$$m_{cd}^{\min} = m_c + m_d, \tag{7}$$

$$m_{cd}^{\max} = M_{\text{mother}} - 2m_{\text{DM}} \qquad \text{[Right process of Eq. (9)]}. \tag{8}$$

Physically, the lower limit corresponds to the case when the two visible particles a, b (and similarly c, d) are at rest in their center-of-mass frame so that they move with the same velocity in any Lorentz frame. The upper limit corresponds to the case in which the DM particle(s) are at rest in the overall center-of-mass frame of the final state. Both maxima are independent of the masses of the virtual intermediate particles. The point is that the upper endpoints in the two distributions are different.

A. Double edge

An especially striking/interesting case is when the SM particles in the two decay chains are identical:

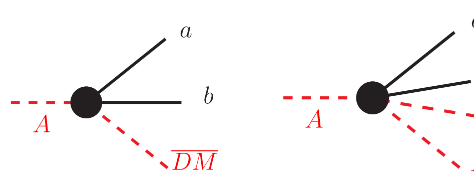

(9)

As we show below, it is possible to obtain a *double* edge in the distribution of this SM final state. We begin with presenting a basic idea of this phenomenon, before going on to more details.

1. Basic idea

Taking into account the fact that the visible particles of both decays are the same and assuming that both subprocesses are allowed, the experimental distribution

---

[2] See Fig. 9 for appearance of these two types of decays, including the required interactions, in the context of an explicit model.

[3] Of course, which of the two particles is denoted anti-DM is a matter of convention. Also, as a corollary, the DM particle should be Dirac fermion or complex scalar in a Z_3 model.

[4] We explore the effects of basic background and detector cuts at the LHC for a simple model in Sec. IVA 2. There we show the effects discussed in this section remain after cuts for the background.

$(1/\Gamma)d\Gamma/dm_{ab}$ will contain events of both processes. In such a combined distribution, clearly, the endpoint of Eq. (8)—denoted now by $m_{ab}^{\prime\,\max}$—will become an *edge* in the middle of the distribution, which along with the overall kinematic endpoint given by Eq. (6), will give rise to a *double edge* signal. Assuming the two edges are visible, it is interesting that we can determine *both* the DM and mother particle masses by simply inverting Eqs. (6) and (8):

$$m_{\mathrm{DM}} = m_{ab}^{\max} - m_{ab}^{\prime\,\max}, \tag{10}$$

$$M_{\mathrm{mother}} = 2m_{ab}^{\max} - m_{ab}^{\prime\,\max}. \tag{11}$$

In particular, the distance between the two edges is identified as the DM mass.

In contrast to the cases just considered, in Z_2 scenarios only one or three DM particles (i.e., not two) are allowed in a single decay chain due to Z_2-charge conservation (unless the process is triggered with an uncharged mother particle [7]). Independently of phase-space considerations, we note that in Z_2 models the decay chain with three DM particles should be highly suppressed with respect to the one DM case. The reason for such an expectation is that a decay with three DM in the final state requires a vertex with *four* (in general different) Z_2-charged particles which is typically absent, at least at the renormalizable level in most models.[5] Therefore, with only one possible decay process (in terms of the number of DM in the final state) we can only observe a single kinematic endpoint in the invariant mass distributions in a Z_2 model.

2. Details

Of course the visibility of such a signal depends on the shapes of the distributions of each subprocess as well as their relative decay branching fractions. The solid curve and the dashed plot in the left panel of Fig. 1 illustrate the generic shape of the distributions for the two processes of Eq. (9) based only on pure kinematics, i.e., no effects of matrix element and spin-correlations. (Such effects might be important and we will return to this issue in the context of specific models to show that multiple edges can still "survive" after taking these effects into consideration.) Because of the phase-space structure of the processes one realizes that the distribution in the case of 3-body decays is more "bent" towards the right (i.e., larger values of invariant mass) whereas for the 4-body decays the peak of the distribution leans more towards the left (i.e., smaller values of invariant mass). Because of this feature, the combination of the two distributions can give rise to two visible *edges* (as long as the relative branchings of the two decays are of comparable size). This is shown in the right panel of Fig. 1 in which we show the combined invariant mass distribution of the two visible SM particles, for three different relative branching fractions of the two subprocesses. Based on the location of the *edges* in right panel of Fig. 1 and Eqs. (10) and (11), the mass of DM particle must be about 300 GeV and the mass of the mother particle must be about 800 GeV, which are of course the masses used in the example.

Whether or not the double-edge signal is clear (and hence we can determine the DM and mother masses) also depends on the DM mass which must be relatively sizable compared to the mass of the mother particle. For example, if we take a DM mass of 50 GeV instead of 300 GeV that we assumed above, with the mother mass fixed at 800 GeV, we observe from Fig. 2 that the plotted distribution does not provide a good measurement of M_{mother} and m_{DM}.

Let us return to the issue of the relative branching fraction for each subprocess. The decay into two DM particles should be generically phase-space suppressed relative to the decay into just one DM particle, So, based on pure phase-space suppression, the branching ratio of the decay into two DM might be much smaller than the decay into one DM (unlike what is chosen in the figures above). Hence, it might be difficult to observe a double-edge signal. However, in specific models this suppression could be compensated by larger effective couplings so that the two decays have comparable branching ratio, and therefore, the double edge is visible as in Fig. 1.

In fact, another possibility is that the two decay chains for the Z_3 case, i.e., with one and two DM particles, do *not* have *identical* SM final states, but there is some overlap between the two SM final states. For example,

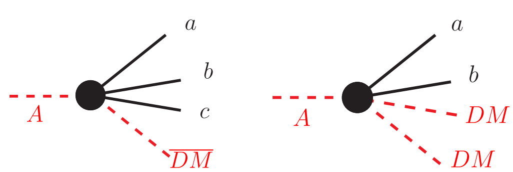

(12)

If we assume that particle c is (at least approximately) massless, then the maximum kinematic endpoint of m_{ab} in the first of the above-given two reactions is still $M_{\mathrm{mother}} - m_{\mathrm{DM}} - m_c \approx M_{\mathrm{mother}} - m_{\mathrm{DM}}$. In this situation *both* the reactions have 4-body final states and hence could be easily have comparable rates, at least based on phase-space [cf. Earlier we had 3-body vs 4-body by requiring the same two-body SM final state for the two reactions found in (9)]. On the other hand, although the two rates are now comparable, it might actually be harder to observe a double edge because the shape of the two individual distributions are both peaked towards the left (i.e., smaller values of invariant mass) and even if they have different endpoints, the combined distribution might not show as clearly a double edge as the earlier case where the two shapes are apparently distinct.

[5] Compare this situation to the Z_3 case, where appearance of two DM in a decay chain comes from vertex with *three* Z_3-charged particles which is more likely to be present, especially at the renormalizable level.

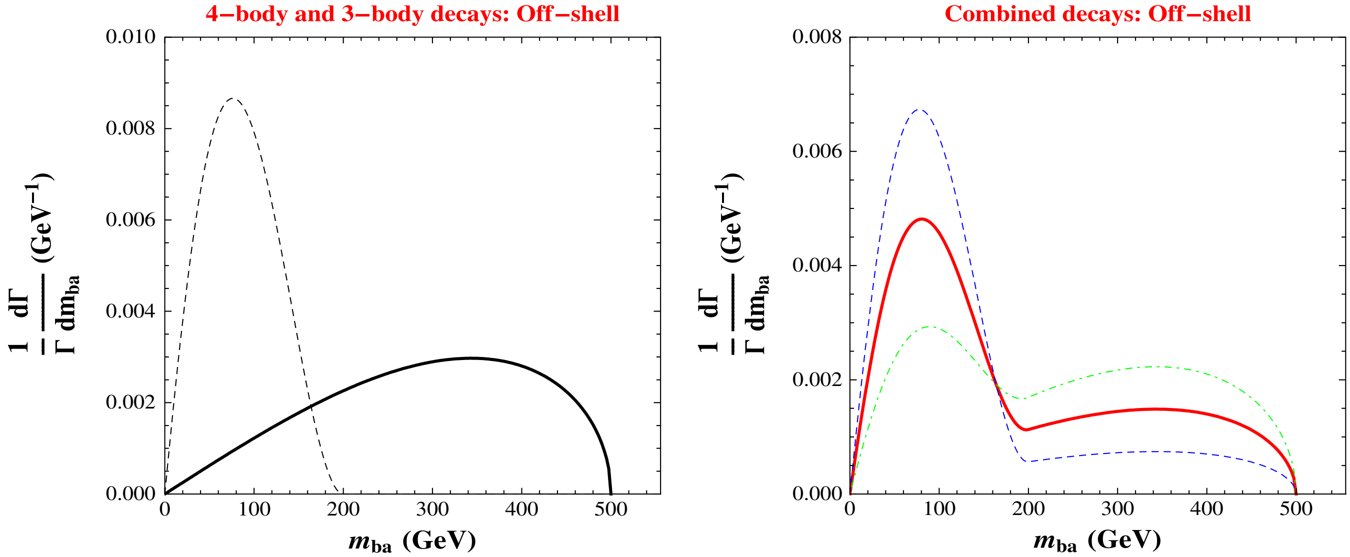

FIG. 1 (color online). Invariant mass distribution $(1/\Gamma)d\Gamma/dm_{ab}$ for the processes of Eq. (9). The masses of the mother particle A and of the DM particles are $m_A = 800$ GeV and $m_{\rm DM} = 300$ GeV and the SM particles a and b are assumed to be massless. The solid and dashed curves on the left panel represent the distributions for the 3-body decay and the 4-body decay, respectively. On the right panel, blue/dashed (highest peaked), red/solid, and green/dot-dashed (lowest peaked) curves show the combined distributions with branching ratios of 3-body to 4-body given by 1:3, 1:1, and 3:1, respectively.

B. Different edges in pair production

Finally, what if there are no common SM particles between the final states of the decay chains with one and two DM particles so that we do not obtain a double edge? In this case, one can consider another analysis, by making the further assumption that the same mother particle A is pair-produced in each event, and that the decay products of each A are now distinct and very light or massless, i.e.,

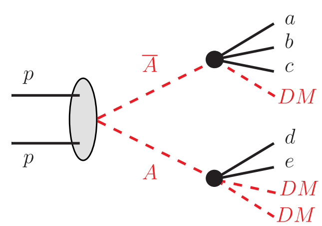

(13)

Here we have chosen three SM particles (a, b, c) in the decay chain with one DM just so that both decay chains involve a 4-body final state. In this situation one can restrict to events with all five SM particles $(a, \ldots e)$ particles in the final state,[6] but use both sides of the event, i.e., obtain the full invariant mass distribution of the visible particles of each (distinct) side. In the interpretation of these results in the context of a Z_3 model, the difference between the endpoints of each separate distribution will give the dark matter mass, and like before, the mass of the mother particle A can be found using a combination of the two endpoints, i.e., $m_{\rm DM} = m_{abc}^{\rm max} - m_{de}^{\rm max}$ and $M_{\rm mother} = 2m_{abc}^{\rm max} - m_{de}^{\rm max}$.

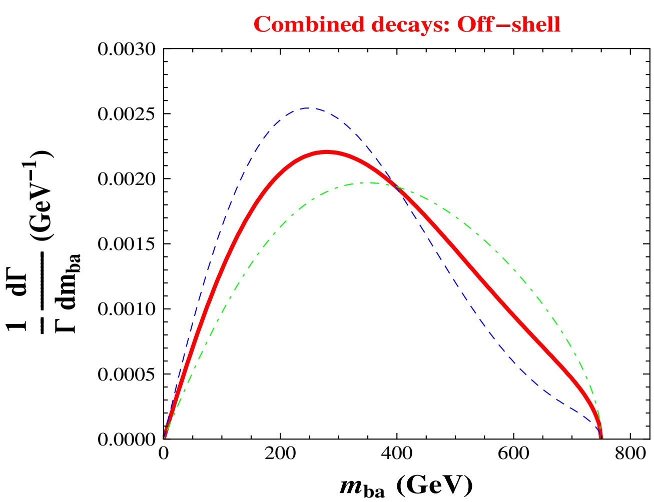

FIG. 2 (color online). Same as the right panel of Fig. 1 but using a smaller DM mass, $m_{\rm DM} = 50$ GeV. The *edge* in the middle of the distribution is no longer apparent.

III. ON-SHELL INTERMEDIATE PARTICLES

In this section, we consider the case where the mother particle decays into SM and DM via intermediate particles which are all *on*-shell. Again, like in Sec. II all particles are assumed to decay inside the detector. In this case, the

[6]If we include other events which have a, b, c or d, e on *both* sides, we still get the different edges that we discuss below, but as we will mention later, such events will not allow us to get rid of "faking" Z_2 models.

endpoints of invariant mass distributions will depend on the masses of these intermediate states as well as the masses of the mother and the final state particles. Both in the Z_2 and Z_3 cases there will be more possibilities for the upper endpoints because of the possibilities of "multiple topologies" and "different intermediate particles" (to be explained below) for the same visible final state. Since even for the Z_2 case it is possible to obtain multiple edges, finding multiple edges is not anymore a robust discriminator between Z_2 and Z_3 unlike the off-shell decay case. We then discuss a topology of the decay chain which does allow us to distinguish between the two models.

A. Additional sources of multiple edges

Here we discuss how it is possible to obtain multiple edges even if we do *not* combine decays of mother particle into one and two DM particles.

1. Multiple topologies

For Z_3 models we can expect multiple endpoints from the decays of the same mother particle into a given SM final state by combining the two decay chains with one DM and two DM particles, respectively, just as in the case of the decays with off-shell intermediate particles. However, this is not the only way of obtaining multiple endpoints, i.e., such a combination of decay chains with one and two DM is not essential. The reason is that there are multiple possible topologies even with the completely identical final state if it contains *two* DM, due to the various possibilities for the locations of two DM particles relative to the other SM particles in a decay chain. For example, for the case of a 4-body decay process (i.e., two SM and two DM particles) there will be *three* different possibilities:

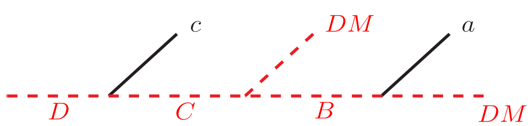

(14)

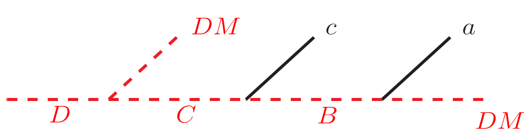

(15)

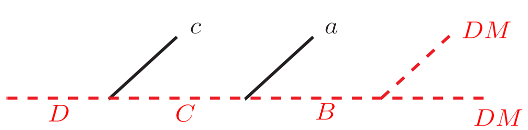

(16)

Note that (as above) decay cascades involve a "charged-charged-charged" (under Z_3 symmetry) vertex (in addition to "charged-charged-neutral" vertices) in order to contain two DM particles in the final state.

Assuming that the visible particles are massless, $m_a = m_c = 0$, the upper endpoints for each topology are given by (See Appendix A for details.):

$$(m_{ca}^{\max})^2 = \frac{2(m_D^2 - m_C^2)(m_B^2 - m_{\rm DM}^2)}{m_B^2 + m_C^2 - m_{\rm DM}^2 - \lambda^{1/2}(m_C^2, m_B^2, m_{\rm DM}^2)} \tag{17}$$

(for Eq. (14))

$$(m_{ca}^{\max})^2 = \frac{(m_C^2 - m_B^2)(m_B^2 - m_{\rm DM}^2)}{m_B^2} \qquad \text{(for Eq. (15))} \tag{18}$$

$$(m_{ca}^{\max})^2 = \frac{(m_D^2 - m_C^2)(m_C^2 - m_B^2)}{m_C^2} \qquad \text{(for Eq. (16))} \tag{19}$$

where λ is the well-known kinematic triangular function given in the form of

$$\lambda(x, y, z) = x^2 + y^2 + z^2 - 2xy - 2yz - 2zx. \tag{20}$$

The main point is that kinematic endpoints are functions of the masses of the mother, the DM and the intermediate particles, and moreover, this dependence changes according to different topologies. Thus, even if the intermediate particles involved in these decays of a given mother particle are the same, one will still obtain multiple endpoints.[7] Finally, if we combine decay chains with one and two DM in the final state (even if the latter has just one topology), the difference between the two endpoints will not lead to a direct measurement of the DM mass like in the off-shell decay case because again, the mass of intermediate particles is one of the main ingredients to determine the endpoints.

In Z_2 models the decay topologies must have a single DM particle and that too at the end of the decay chain because the vertices in the decay cascade are of the form "odd-odd-even" (under the Z_2 symmetry).[8] Nevertheless, there can still be different topologies because of different ordering of the visible states. For example:

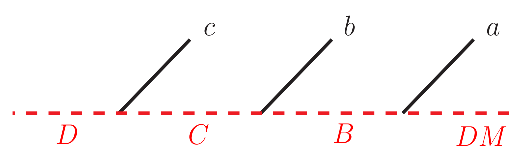

(21)

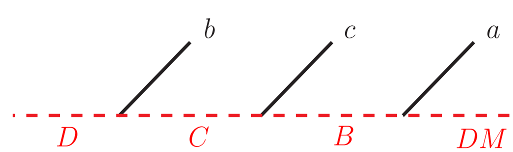

(22)

⋮

Obviously, the endpoints for a given invariant mass distri-

[7]Of course, the different possible decay topologies can, in general, have different intermediate states.

[8]Note that a similar argument applies to decay chains in Z_3 models with only *one* DM in the final state.

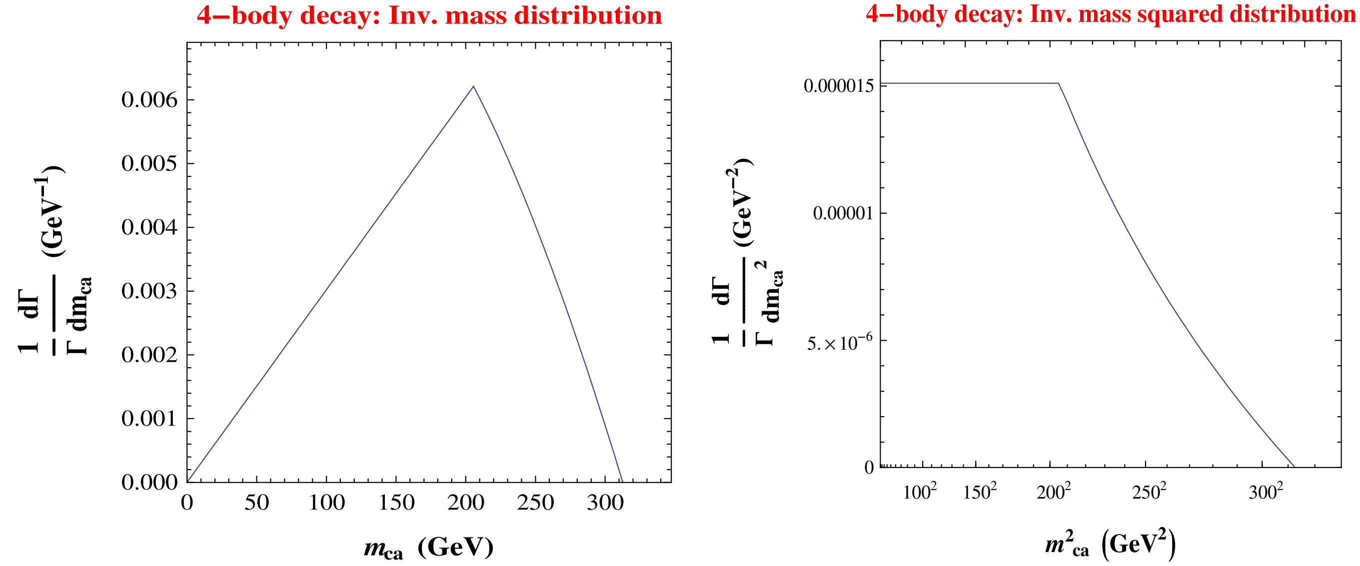

FIG. 3 (color online). The panel on the left shows the distribution in m_{ca} while the right-hand panel shows the distribution in m_{ca}^2 from the decay chain of Eq. (24). The masses of mother particle, two intermediate particles, and DM particles are 800 GeV, 700 GeV, 400 GeV, and 200 GeV, respectively, and the SM particles are assumed massless. A cusp due to the topology of Eq. (24) is clear in both distributions.

bution, say m_{ca}, will be different for each of these two topologies, and actually they can be obtained from Eqs. (17) and (18) by just replacing $m_{\rm DM}$ in the denominator of Eqs. (17) by m_b and leaving Eqs. (18) unchanged (and where m_a and m_c are still assumed to vanish).

2. *Different intermediate particles for same final state*

In addition, even if the topology and the order of visible particles are the same, there is the possibility of multiple paths for the *same* mother particle to decay into the same (SM and DM) final state by involving different intermediate particles. We will obtain multiple endpoints in this case because of the dependence of the endpoints on the masses of intermediate particles (as mentioned above). This argument is valid for both the Z_2 and Z_3 models (and one or two DM for the latter case): for a final state with two SM and one DM, we can have

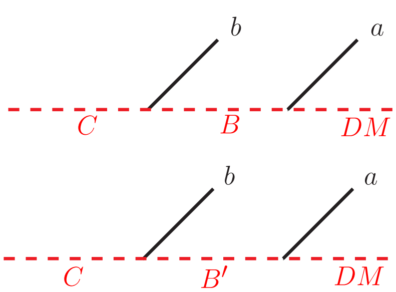

(23)

For example, in SUSY, the decay chain $\chi_2^0 \rightarrow l^+ l^- \chi_1^0$ can proceed via intermediate right- or left-handed slepton. Since the masses of intermediate right- and left-handed sleptons are in general different, multiple endpoints are expected.

B. Cusp topology

So far, we have learned that for on-shell intermediate particle cases the multiple edge signal is not a good criterion to distinguish Z_3 from Z_2. Instead, we focus on *shapes* of these distributions. Consider the topology which can be present in Z_3 models (but absent in the Z_2 case) with two visible SM particles separated by a DM particle,[9] i.e.,

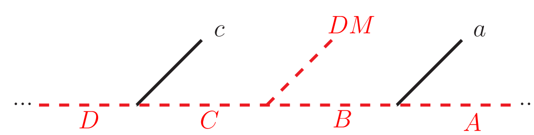

(24)

We assume massless SM particles (i.e., $m_a = m_c = 0$) and the mass hierarchy $m_D > m_C > m_B > m_A$. Also, we neglect spin-correlation effects in this section. We sketch the derivation of the distribution of the ac invariant mass here and refer the reader to the Appendix A for details. The differential distribution $\frac{1}{\Gamma}\frac{\partial \Gamma}{\partial m_{ac}^2}$ that we want to study can be obtained for this "new" topology easily by noting that the differential distribution $\frac{1}{\Gamma}\frac{\partial^2 \Gamma}{\partial u \partial v}$ must be flat, where the variables are defined as follows

$$u = \frac{1 - \cos\theta_{c\rm DM}^{(C)}}{2} \quad \text{and} \quad v = \frac{1 - \cos\theta_{ca}^{(B)}}{2}, \tag{25}$$

[9] Note that in general D might come from the decay of another Z_3-charged particle and similarly, at the end of the decay, A might not be the DM, that is, it could itself decay further into DM particles and other visible states as long as Z_3-charge conservation is respected. The "..." to the left of D and to the right of A signify this possibility.

with $\theta_{ca}^{(B)}$ being the angle between c and a in the rest frame of B, and $\theta_{c\mathrm{DM}}^{(C)}$ being the angle between c and DM in the rest frame of C [21]. In addition, we have $0 < u,\ v < 1$. Thus, we can write

$$\frac{1}{\Gamma}\frac{\partial^2\Gamma}{\partial u \partial v} = \theta(1-u)\theta(u)\theta(1-v)\theta(v) \tag{26}$$

One further finds that

$$m_{ca}^2 = m_{ca}^{\max}(1-\alpha u)v, \tag{27}$$

where $m_{ca}^{\max}$ is given in Eq. (17) with m_{DM} in the numerator replaced by m_A, and so we can make a change of variables from the differential distribution of Eq. (26) and obtain the distribution $\frac{1}{\Gamma}\frac{\partial^2\Gamma}{\partial u \partial m_{ca}^2}$, which can then be integrated over u to finally obtain the distribution with respect to m_{ca}[10]:

$$\frac{1}{\Gamma}\frac{\partial\Gamma}{\partial m_{ca}} = \begin{cases} \frac{2m_{ca}}{(m_{ca}^{\max})^2\alpha}\ln\frac{m_C^2}{m_B^2} & \text{for } 0 < m_{ca} < \sqrt{1-\alpha}m_{ca}^{\max} \\ \frac{2m_{ca}}{(m_{ca}^{\max})^2\alpha}\ln\frac{(m_{ca}^{\max})^2}{m_{ca}^2} & \text{for } \sqrt{1-\alpha}m_{ca}^{\max} < m_{ca} < m_{ca}^{\max} \end{cases} \tag{28}$$

where $m_{ca}^{\max}$ is given in Eq. (17) and

$$\alpha = \frac{2\lambda^{1/2}(m_C^2, m_B^2, m_{\mathrm{DM}}^2)}{m_B^2 + m_C^2 - m_{\mathrm{DM}}^2 + \lambda^{1/2}(m_C^2, m_B^2, m_{\mathrm{DM}}^2)}. \tag{29}$$

From these results we can easily see that the new topology introduces two different regions in the m_{ca} distribution with a cusp at the boundary connecting both regions, located at $\sqrt{1-\alpha}m_{ca}^{\max}$. Figure 11 shows the same distribution in both panels, but with respect to m_{ca} on the left panel and with respect to m_{ca}^2 on the right panel. As we will argue later, the second option seems better suited once spin correlations are taken into account, but in both plots, one observes that the cuspy feature is quite clear.

1. Two visible particles

Consider first the simple case of *only* two visible particles in a decay chain. In the Z_3 reaction of Eq. (24), D is then the mother particle and A is DM. Clearly, we would find a cusp in the invariant mass distribution of the two visible particles in the Z_3 model, but not for the Z_2 model since the two visible particles must always be adjacent to each other in the latter case.[11] Thus, the presence/absence of cusp could be used to distinguish Z_3 and from Z_2 models.

[10]Note that $\frac{1}{\Gamma}\frac{\partial\Gamma}{\partial m} = 2m\frac{1}{\Gamma}\frac{\partial\Gamma}{\partial m^2}$.

[11]Note that we are considering decay of a Z_3 or Z_2-*charged* mother. A Z_2-uncharged, i.e., *even*, mother *is* allowed to decay into two DM and can give a cusp in the invariant mass of two visible particles from such a decay [7].

2. Generalization to more than two SM particles in decay chain

Of course, in general in both Z_2 and Z_3 models there will be more than two visible particles with possibly some of them being identical, and this will undoubtedly complicate the analysis. For example, in the reaction of Eq. (24), a, c, or both can be produced at some other place of the same decay chain in addition to the locations shown there, e.g.,

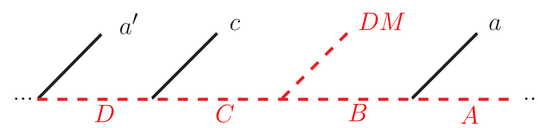

(30)

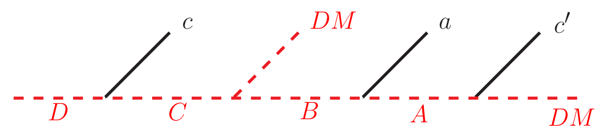

(31)

Here a', which is an identical particle to a, is assumed to come from the immediate left of D, and c', which is an identical particle to c, is assumed to come from the immediate right of A. Note that there is no DM between a' and c (unlike between a and c) in first reaction above (similarly between a and c' vs between a and c in second reaction above), and that a and a', and c and c' are identical. Therefore, in both these examples, it is clear that we will obtain a more complicated distribution in m_{ac} than the one studied previously.

Nevertheless, the method described previously to disentangle the Z_2 from the Z_3 cases (when having two visible particles), can still be generalized to the situation of many visible particles in a decay chain. For example, let us consider the case of *three* visible SM particles in the final state for both Z_3 and Z_2 models. We will obtain a cusp even in the Z_2 case when considering the invariant mass of two *not* "next-door neighbor" visible particles such as in m_{ac} for the decay process in Eq. (21). The reason is that, even though the precise topology of Eq. (24) is absent in a Z_2 model, a similar one is generated by the presence of a SM particle (i.e., b) in-between two other SM particles (i.e., a and c) as in Eq. (21). Thus the analysis performed earlier for Eq. (24) applies in this case, but with the DM mass set to zero (assuming SM particle b is massless).

However, this type of degeneracy between Z_2 and Z_3 can be resolved by considering all of the three possible *two-(visible) particle* invariant mass distributions. In the Z_3 case with two DM particles in the final state, two of these three invariant mass distributions will have cuspy features whereas only one such invariant mass distribution will have a cusp in the Z_2 case. The reason is again that in the Z_3 case, since one more particle is added to the decay products compared to the Z_2 case (i.e., we have two invisible and three visible particles), there will be final state particles (visible or not) in between the two visible particles for two of the three pairings. This feature remains true for more visible particles, i.e., in general we will obtain more cusps in the invariant mass distributions in a Z_3 model than in a Z_2 model.

C. Spin correlations

Once spin correlations are involved, the derivative discontinuity (cusp) might appear unclear. Nevertheless, it may still be possible to distinguish a Z_3 model from a Z_2 model by employing the fitting method which we will show in the rest of this section. The basic idea is that the distribution $d\Gamma/dm_{ca}^2$ of three-body decays in Z_2 (i.e., one DM particle and two visible particles) can (almost) always be fitted into a quadratic function in m_{ca}^2, whereas the distribution of the new topology of Z_3 cannot not be fitted into a single quadratic function, that is, two different functions are required for fitting each of the two subregions of the distribution. Let us see how this works for a Z_2 model (i.e., one DM and two visible particles) and a Z_3 model (i.e., two DM and two visible particles) in turn.

1. Z_2 *case: 1* DM + 2 *visible*

We can again make use of the same angular variables considered earlier for the case of this 3-body decay cascade, shown, for example, in Eq. (23). According to Refs. [21,22], the normalized distribution including spin correlations is given by

$$\frac{1}{\Gamma}\frac{\partial\Gamma}{\partial t} = \theta(t)\theta(1-t)f(t) \tag{32}$$

where again we have defined the variable t as

$$t \equiv \frac{1-\cos\theta_{ba}^{(B)}}{2}. \tag{33}$$

Here $f(t)$ is a function of t and $\theta_{ba}^{(B)}$ is the angle between particles a and b of Eq. (23) in the rest frame of particle B. One then notes that $m_{ba}^2 = (m_{ba}^{\max})^2 t$ which basically means that the distribution with respect to the invariant mass m_{ba}^2 (which is of our interest) is essentially the same as the one with respect to t above. This means that the distribution in m_{ba}^2 will have the functional form f. According to Ref. [23], such spin correlation functions are just polynomials of $\cos\theta_{ba}$ (i.e., $(1-2t)$). Moreover, if we restrict our consideration to particles of spin-1 at most, the maximum order in t of the polynomial is two, which means that the most general form of f will be

$$f(t) = c_1 + c_2 t + c_3 t^2. \tag{34}$$

In turn, the invariant mass distribution we are interested in must therefore take the form (in the region between the endpoints enforced by the θ-functions)

$$\frac{1}{\Gamma}\frac{d\Gamma}{dm_{ba}^2} = c_1' + c_2' m_{ba}^2 + c_3' m_{ba}^4. \tag{35}$$

With the experimental data we can construct the invariant mass distribution, and we will be able to determine the three constants c_1', c_2', and c_3' by fitting into a parabola in the m_{ba}^2 variable. In other words, for any 3-body decay chain, with or without spin correlation, it is always possible to fit the invariant mass distribution $\frac{1}{\Gamma}\frac{d\Gamma}{dm_{ba}^2}$ into a curve quadratic in m_{ba}^2.

2. Z_3 *case: 2* DM + 2 *visible*

We now consider the new topology of Eq. (24) including the possibility of spin correlations. As in Sec. III A, we use the same angular variables u and v. However, the normalized distribution with spin correlations become a little more complicated than before

$$\frac{1}{\Gamma}\frac{\partial^2\Gamma}{\partial u\partial v} = \theta(v)\theta(1-u)g(u)\theta(v)\theta(1-v)h(v) \tag{36}$$

where again

$$u \equiv \frac{1-\cos\theta_{c\mathrm{DM}}^{(C)}}{2}, \qquad v \equiv \frac{1-\cos\theta_{ca}^{(B)}}{2}. \tag{37}$$

Like in the previous section, $g(u)$ and $h(v)$ are spin-correlation functions (cf. $g = h = 1$ without spin correlation discussed earlier) and again the invariant mass squared is given by

$$m_{ca}^2 = (m_{ca}^{\max})^2(1-\alpha u)v. \tag{38}$$

where α is the same kinematical constant defined in Eq. (29). As in the analysis without spin correlations, the two types of θ-functions will split the entire region into two subregions, with a cusp at the separation point, whose location is independent of the spin-correlation effects (since it depends on purely kinematical constants α and $m_{ca}^{\max}$). But unlike the scalar case (i.e., with no spin correlations), we have now two functions $g(u)$ and $h(v)$, which can change the shape of the distribution and in principle affect the derivative discontinuity (the cusp).

In detail, by the chain rule the previous normalized distribution can be modified and partially integrated to obtain

$$\frac{1}{\Gamma}\frac{d\Gamma}{dm_{ca}^2} = \int_0^{u_{\max}} \frac{du}{(m_{ca}^{\max})^2(1-\alpha u)} g(u) h\left(\frac{m_{ca}^2}{(m_{ca}^{\max})^2(1-\alpha u)}\right) \tag{39}$$

where

$$u_{\max} = \mathrm{Max}\left[1, \frac{1}{\alpha}\left(1-\frac{m_{ca}^2}{(m_{ca}^{\max})^2}\right)\right]. \tag{40}$$

The two possible choices in the definition of $u_{\max}$ above arise when integrating $\frac{1}{\Gamma}\frac{\partial^2\Gamma}{\partial m_{ca}^2\partial u}$ with respect to u due, in turn, to the integration limits enforced by the θ functions. This leads to two different regions for the differential distribution such that in the first subregion, we have $0 < m_{ca} < \sqrt{1-\alpha}m_{ca}^{\max}$ and $u_{\max} = 1$, while for the second region, we have $\sqrt{1-\alpha}m_{ca}^{\max} < m_{ca} < m_{ca}^{\max}$ and $u_{\max} = \frac{1}{\alpha}(1-\frac{m_{ca}^2}{(m_{ca}^{\max})^2})$ [21]. So far, most of the steps are similar to the case of no spin correlations except for the presence of the factors of spin-correlation functions, g and h.

It would seem that we need to know the *precise* form of g and h in order to proceed further, i.e., in order to perform the integration in Eq. (39). However, for the purpose of determining whether or not there is a cusp, we will show that it is sufficient to know the fact that those spin-correlation functions must be second order polynomials in their argument as mentioned in the analysis of the Z_2 case. Using this fact we can write down the above integrand as

$$\frac{1}{1-\alpha u} g(u) h\left(\frac{t}{1-\alpha u}\right) = \frac{b_1}{(1-\alpha u)^3} t^2 + \frac{1}{(1-\alpha u)^2} \times (b_2 t + b_3 t^2) + \frac{1}{1-\alpha u} \times (b_4 + b_5 t + b_6 t^2) + (b_7 + b_8 t) + b_9(1-\alpha u), \tag{41}$$

where we have introduced the same variable $t \equiv m_{ca}^2/(m_{ca}^{\max})^2$ used for the 3-body decays and where the kinematical constants b_i will depend on the specific nature of the couplings and particles in the decay chain (i.e., they must be calculated on a case by case basis). The terms of the integrand are organized as a power series in $(1-\alpha u)$—instead of in u—because of the simplicity of the former form. Integrating then gives

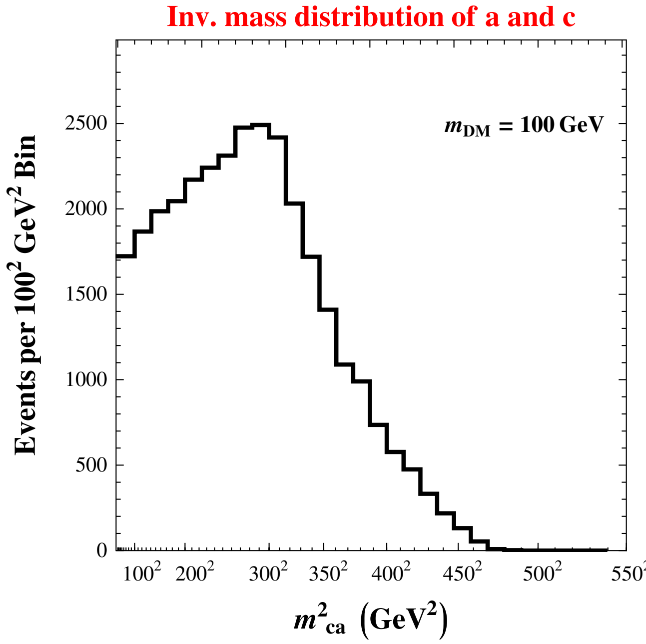

FIG. 4 (color online). Invariant mass distribution of particles a and c, from the decay chain shown in Eq. (24), including spin correlations, and such that the intermediate particle C has spin 1 and the intermediate particle B has spin $1/2$, and the couplings are chiral. The cusp in this distribution appears more defined than in Fig. 3 where spin correlations were not considered.

$$\frac{1}{\Gamma}\frac{d\Gamma}{dt} = \begin{cases} b_1' + b_2' t + b_3' t^2 & \text{for } 0 < t < \sqrt{1-\alpha} \\ b_1'' + b_2'' t + b_3'' t^2 + (b_4'' + b_5'' t + b_6'' t^2)\log t & \text{for } \sqrt{1-\alpha} < t < 1 \end{cases} \tag{42}$$

where again, the kinematical constants b_i' and b_i'' are specific to each situation. Thus, even with spin correlations, the functional dependence on $t(\propto m_{ca}^2)$ is quite simple; however, the crucial point is that it is different for each subregion of the distribution. In particular this simple dependence in the distribution of m_{ca}^2 (and *not* m_{ca}) suggests that it may be more appropriate to consider the distribution of m_{ca}^2 instead of the distribution of m_{ca}. In Fig. 4 we show the m_{ca}^2 invariant mass distribution for the decay chain of Eq. (24), but in the special case where particle C has spin 1 and the intermediate particle B is a fermion, and some of the couplings are chiral. We used MADGRAPH [24] to generate events taking the particles a and c to be massless and taking $m_{\mathrm{DM}} = 100$ GeV. One can compare the shape of this distribution with the one from the right panel of Fig. 11 and see that in this case, including the spin correlation makes the cusp even more apparent.

One of the main differences between the two subregions is that the first one has no logarithmic dependence in t while the second (in general) does have it. Of course, from Eq. (41), we see that this logarithmic term could be suppressed for the case $b_4 = b_5 = b_6 \sim 0$. However, even in this special case we would still have to employ different sets of coefficients in the two subregions as follows. The functional forms in both the regions are now quadratic in t, i.e.,

$$\frac{1}{\Gamma}\frac{d\Gamma}{dt} = \begin{cases} b_7 + \frac{b_9}{2}(2-\alpha) + \left(\frac{b_2}{1-\alpha} + b_8\right)t + \left[\frac{b_1(2-\alpha)}{2(1-\alpha)^2} + \frac{b_3}{1-\alpha}\right]t^2 & (0 < t < \sqrt{1-\alpha}) \\ \frac{1}{\alpha}\left[b_2 + b_7 + \frac{b_1+b_9}{2} - (b_2 - b_3 + b_7 - b_8)t - \left(b_3 + b_8 + \frac{b_1+b_9}{2}\right)t^2\right] & (\sqrt{1-\alpha} < t < 1) \end{cases} \tag{43}$$

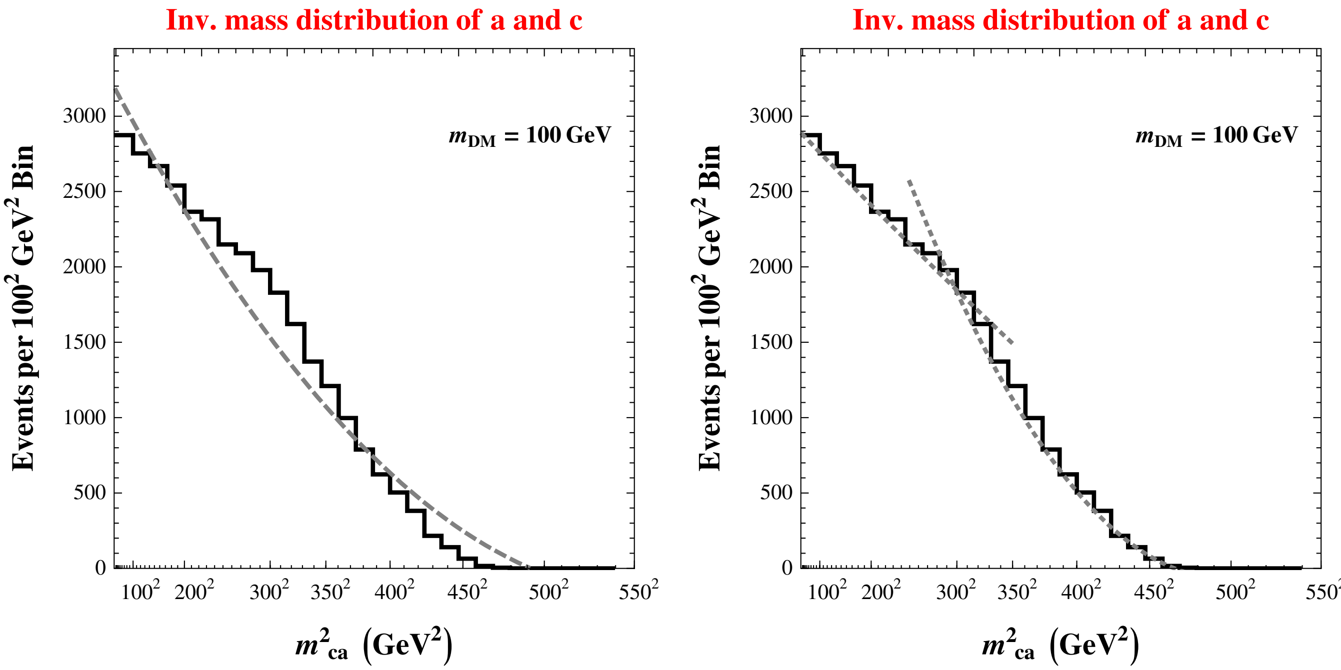

FIG. 5 (color online). Invariant mass distribution of particles a and c, as in Fig. 4, but with different chiral couplings. The cusp position is less apparent in this case but one can see (left panel) that a fit to a polynomial of second order as shown in Eq. (35) is not very good (that is, the Z_2 interpretation). On the right panel we show the same distribution, with a different fitting function for the left side of the distribution and the right side [see Eq. (42)], consistent with the existence of a cusp, i.e., the Z_3 interpretation.

Considering just the constant terms, we see that it is possible to obtain identical functions in the two regions only if $\alpha = 1$ and $b_1 = b_2 = 0$. However, using Eqs. (20) and (29), it can be shown that α is always (strictly) less than 1. In other words, it is highly unlikely that the distribution in each subregion can be fitted successfully to the same polynomial of order two in t; the cusp will thus survive even in this case.

In Fig. 5 we show the distribution (again obtained with MADGRAPH [24]) for the same decay chain as in Fig. 4, but where the chiral structure of some couplings has been modified from before. We see that the cusp feature is now less apparent, but one also sees that a full fit to a polynomial of order two (left panel) is not as good as a *multiple-region* fit (right panel), where the first part of the distribution is fitted to a polynomial of order two [see first line of Eq. (42)], and the right side of the distribution is fitted to the functional form (with a logarithm) given in the second line of Eq. (42).

IV. EXAMPLE MODELS

A. Stabilization symmetries from spontaneous symmetry breaking

The most popular models of physics beyond the SM focus on solving the weak-Planck hierarchy problem by adding new particles at the *weak* scale. Some of these new particles can be stable as a consequence of a discrete (often a parity) symmetry that is a part of (or imposed on) the theory. Thus these particles can have the correct thermal relic abundance to constitute dark matter, i.e., dark matter is then a "spin-off" of solving the hierarchy problem. It may be possible, however, that the question of the origin of dark matter is not rooted in *first* solving the hierarchy problem. In this case, it is the thermal relic density which "fixes" the mass of the dark matter particles to the weak scale. As well, it is also known that the dark matter and baryon densities today are close in size

$$\Omega_{\mathrm{DM}} \sim 4.7\Omega_{\mathrm{baryon}} \tag{44}$$

which provides a hint to a possible common origin which may have a solution at the weak scale.

With this background, in Ref. [15], a model was introduced in which a $SU(N)$ gauge group is spontaneously broken to the Z_N center. There the goal was to, in part, determine whether a "copy" of weak interactions could generate a viable dark matter candidate. As is well known, the SM electroweak gauge group is spontaneously broken to $U(1)_{\mathrm{em}}$ which makes the lightest electrically charged particle (i.e., the electron stable). By analogy the $SU(N)$ gauge group in this model is broken to the Z_N center that stabilizes dark matter. The dark matter candidates which transform, e.g., as a fundamental under the $SU(N)$ are stabilized by the Z_N. A unique, testable feature of these models is the existence of new gauge bosons that are neutral under the SM symmetries but do not couple to SM particles as Z bosons. These gauge bosons transform as adjoints under the $SU(N)$ and therefore are invariant under the Z_N center.

The fermionic dark matter candidate mentioned above [i.e., transforming as a fundamental under $SU(N)$] would get a mass $m \sim \lambda v_{\text{new}}$. Here λ is a generic $\mathcal{O}(1)$ Yukawa coupling. For this mass to be of order the weak scale as required for the thermal relic abundance [15], the vacuum expectation value (vev) that breaks the $SU(N)$ must be of order the SM Higgs vev. Thus, the $SU(N)$ gauge bosons also have weak scale masses. As a *bonus* (or "double-duty") of the new $SU(N)$ vev being similar to the Higgs vev, at finite temperature these gauge bosons have sphaleron solutions and nucleate additional bubbles (in analogy with the weak interactions) that may be relevant for electroweak baryogenesis.

Let us make a connection to our study of distinguishing Z_3 from Z_2 using double edges described in Sec. II and new topologies described in Sec. III. There, we chose Z_3 symmetry mainly for illustration; in any case, the key to our signal is the existence of "charged-charged-charged" couplings under the dark matter stabilization symmetry in the decay chain. Parity stabilized models have only "odd-odd-even" couplings. Any model, not necessarily a Z_3, that features such coupling has the potential to generate the signals we discussed earlier.

To this end, we take a "toy" limit of the model discussed in Ref. [15]. Namely, we consider a scenario where the new gauge bosons are long-lived and register as missing energy ($\not{E}_T$) in the detectors so that they behave *effectively* as dark matter particles, i.e., as "charged" (even though they were uncharged "to begin with"). This assumption will then "convert" the "dark" $SU(N)$ gauge coupling of a $SU(N)$ fundamental fermion into an effective "charged-charged-charged" coupling which will result in the double kinematic edges as well as the new topologies discussed earlier. The result will also be to generate a hybrid of the on- and off-shell scenarios presented above.

Here, we simply want to make an estimate of the robustness of the signal described in Secs. II and III in the presence of basic detector and background cuts. So, the above toy limit of model in Ref. [15] will suffice for such a study of exploring the effects of the "charged-charged-charged" coupling in a more realistic situation than considered in earlier sections.[12] As a first step, following [15], we summarize the effective lagrangian for our model. Later we will discuss a simple production mechanism and discuss cuts consistent with the ATLAS and CMS collaborations. Results follow afterwards.

For simplicity we chose $N = 2$ to make our analysis. To break the $SU(2)_D \to Z_2$ we require two new additional higgses in the dark sector which transform as an adjoint

$$\phi = \begin{pmatrix} \phi_2 \\ \phi_0 \\ \phi_1 \end{pmatrix} \qquad \eta = \begin{pmatrix} \eta_0 \\ \eta_1 \\ \eta_2 \end{pmatrix}. \tag{45}$$

The Higgs generate the following vevs

$$\phi = \begin{pmatrix} 0 \\ v_1 \\ 0 \end{pmatrix} \qquad \eta = \begin{pmatrix} v_2 \\ 0 \\ 0 \end{pmatrix}. \tag{46}$$

which break the $SU(2)_D$ to the center. A general scalar potential does not naively generate the required breaking. To get the correct vacuum alignment, we require a scalar potential in the dark sector to minimizes $\phi \cdot \eta$. $SU(2)_D$ scalar potential is

$$\begin{aligned} V = {} & \lambda_1(\phi^2 + \lambda_7\phi \cdot \eta - v_1^2)^2 + \lambda_2(\eta^2 + \lambda_8\phi \cdot \eta - v_2^2)^2 \\ & + \lambda_3(\phi^2 + \eta^2 - v_1^2 - v_2^2)^2 + \lambda_4(\phi \cdot \eta)^2 \\ & + \lambda_5\phi^3 + \lambda_6\eta^3. \end{aligned} \tag{47}$$

which generates three new heavy gauge bosons as well as three additional Higgses. In addition, we add anomaly free scalar and fermions with the quantum numbers listed in Table I.

Constructing a supersymmetry UV completion to this effective Lagrangian is straightforward. Although the details is beyond the scope of this paper, note a simple way to do so would be to augment minimum supersymmetric standard model with chiral superfields with the charges in Table I. SUSY breaking terms would then need to be constructed to lift the appropriate particles which will be integrated out to generate the effective theory.

1. Production rates at the LHC

As an example of the unique decay topologies generated by these models, we consider pair production of new exotic heavy quarks, $pp \to \bar{Q}Q$. The leading production mechanism is via QCD

TABLE I. An effective, anomaly free particle spectrum that fills out a $(5, 2) + (\bar{5}, 2)$. The "s" prefactor denotes a scalar particle. Here V_μ are the $SU(2)_D$ gauge bosons. We assume the mass of the Q and sχ is heavy and integrated out. The rest of the spectrum mediates the decay chain in Eq. (48).

Particle	$SU(3)_c$	$SU(2)_L$	$SU(2)_D$	$U(1)_Y$
Q	3	1	2	1/3
sQ	3	1	2	1/3
L	1	2	2	−1/2
sL	1	2	2	−1/2
χ	1	1	2	0
$s\chi$	1	1	2	0
V_μ	1	1	3	0
ϕ	1	1	3	0
η	1	1	3	0

[12] Alternatively, extensive model building along the lines of Ref. [15], which is not the focus of this paper, can provide a "genuine," i.e., without assuming long-lived gauge bosons, "-charged-charged-charged" coupling.

$$pp \to sQ^* sQ + X \to \bar{q}\chi sQ + X \to \bar{q}\chi q\bar{q}l\bar{\chi} + X \quad (48)$$

where X represents the beam remnant and other possible hadronic activity. The first sQ decays via $sQ^* \to \bar{q}\chi$ and the second decay to $sQ \to q\bar{l}l\bar{\chi}$ which is a primary decay chain of study. The charged leptons are $l = e,\ \mu$. The signal is for two isolated leptons, two light quark jets and large amounts of $\not{E}_T$. We take a mass spectrum of

$$\begin{aligned} m_Q &= 700\ \text{GeV} \qquad m_L = 650\ \text{GeV} \\ m_{sL} &= 300\ \text{GeV} \qquad m_\chi = 100\ \text{GeV} \\ m_V &= 100\ \text{GeV} \end{aligned} \quad (49)$$

The topology of the primary decay chain is shown in Fig. 6. The partial decay widths for the sQ is

$$\Gamma_1 = \frac{\lambda_1^2 M_Q}{16\pi}\sqrt{1 - \frac{M_{\rm DM}^2}{M_Q^2}} \qquad \Gamma_2 = \frac{\lambda_2^2 M_Q}{16\pi}\sqrt{1 - \frac{M_L^2}{M_Q^2}} \quad (50)$$

In the analysis, for simplicity, we set all of the Yukawa couplings to $\lambda_1 = \lambda_2 = \lambda$. We assume a 100% branching fraction of $L \to l$sL and sL $\to l\chi$. In this model the gauge boson decays at one loop. sL is the lightest partner; thus, fastest the decay rate goes as

$$\Gamma \sim \frac{g^2\lambda^4}{16\pi^2}\frac{m^{13}}{M^8 M_\chi^4} \quad (51)$$

where m, M_χ and M are the masses of the gauge boson, dark matter, and sL, respectively. Here λ is the coupling between the sL, χ, and the SM lepton. We take λ to have a technically natural value of $\lambda \sim 0.001$ so the gauge boson is long-lived. With the masses given in Eq. (49), we have a lifetime of about 10^{-8} seconds. It should be noted that long-lived particles take about $\sim\mathcal{O}(1) \times 10^{-9}$ seconds to transverse the larger ATLAS detector. Thus, these gauge bosons will register as missing energy. Even though the coupling is so small, the decay chain proceeds because of the branching fractions. Finally, the signal is generated with the new gauge bosons, V, being emitted from the decay chain in Fig. 6. We list the topologies generated to order α in Eqs. (B1)–(B5) in Appendix B. In Secs. II and III, we have discussed the invariant mass distributions for dark matter stabilized with a Z_2 or Z_3 stabilization symmetry with the virtual particles, respectively, off- or on-shell. The present model presents a hybrid between the two pictures. This is because emitting the long-lived gauge boson forces part of the decay chain off-shell. Emitting the new gauge boson also causes these diagram to be

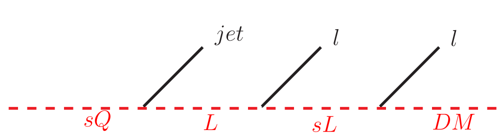

FIG. 6 (color online). The topology of the primary decay chain. Here DM is the χ particle.

suppressed because the virtual particles in the decay chain must go off-shell. Because there are three new gauge bosons, the overall off-shell suppression is enhanced by a multiplicity factor for each boson emitted.

2. Extracting the signal

To get an estimate on the signal we first impose basic acceptance cuts which are consistent with ATLAS and CMS studies of on- as well as off-shell SUSY decay chains. [13,14] We require

$$|\eta_l| < 2.5, \qquad |\eta_j| < 2.5, \quad (52)$$

$$\Delta R_{ll} > 0.3, \qquad \Delta R_{lj}, \Delta R_{jj} > 0.4. \quad (53)$$

where l and j are lepton and jets. η_a is the pseudorapidity of particle a. ΔR_{ab} is defined as $\Delta R_{ab} = \sqrt{d\eta_{ab}^2 + d\phi_{ab}^2}$ where $d\eta_{ab}$ and $d\phi_{ab}$ is the difference in the pseudorapidity and transverse angle of the detector between particles "a" and "b." As described in the previous section, our example signal has two leptons and jets as the SM final states. The primary SM background for this signal is $\bar{t}t$ decays into two leptons. Additional backgrounds include QCD, W + jets and Z + jets events. ATLAS and CMS places additional cuts to reduce this as well as other SM backgrounds. The model allows same-sign or opposite-sign dileptons in the final state. Since the purpose of this section is to see the effect of the detector cuts on our signal, we choose the more conservative opposite-sign dilepton cuts. We adopt cuts consistent with both collaborations by requiring

(1) Two leptons with $p_T > 20$ GeV
(2) At least one leading jet with $p_T > 100$ GeV and subleading jets with $p_T > 50$ GeV
(3) $\not{E}_T > 100$ GeV and $\not{E}_T > 0.2M_{\rm eff}$
(4) Transverse sphericity $S_T > 0.2$.

Here the missing energy ($\not{E}_T$) is defined as

$$\vec{\not{E}}_T = \vec{\not{p}}_T = -\sum_i \vec{p}_{iT} \quad (54)$$

and i runs over the transverse momentum p_T of the visible final state particles in the event. The effective transverse mass $M_{\rm eff}$ is defined as

$$M_{\rm eff} = \sum_i E_{iT} + \not{E}_T \quad (55)$$

where the sum runs over the measured transverse energy E_T from the visible particles in the event. Finally, the transverse sphericity (S_T) is defined as

$$S_T = \frac{2\lambda_2}{\lambda_1 + \lambda_2} \quad (56)$$

where $\lambda_{1,2}$ are the eigenvalues of the 2×2 sphericity tensor

TABLE II. SM backgrounds as computed by [13].

Background	Events (1 fb^{-1})
$t\bar{t}$	81.5
W + jets	1.97
Z + jets	1.20
QCD	0
Total SM	84.67

$$S_{ij} = \sum_{\kappa} p_{\kappa i} p^{\kappa j} \tag{57}$$

where κ runs over the number of final state jets and leptons. The other indices, i and j, run over the p_T components of each particle. S_{ij} is evaluated for the final states with $\eta < 2.5$ and $p_T > 20$ GeV. $S_T \sim 1$ for approximately spherical events; QCD events are usually back-to-back with $S_T \sim 0$. Generally, because our signal has three dark matter candidates per event, these cuts could be optimized with larger $\not{E}_T$ cuts. For direct comparison with ATLAS and CMS, we simulated our signal with the cuts above. The ATLAS collaboration [13] finds the following backgrounds for 1 fb^{-1} of integrated luminosity (see Table II).

In addition to these backgrounds, we have an additional irreducible background when the Z_2-like signal process, Eq. (48), emits Z boson which decay invisibly. The invisible branching for Z bosons into neutrinos is 20% [25]. Finally, in our analysis we simulate calorimetry responses for the energy measurements by adopting Gaussian smearing [13] with the following parameters.

$$\frac{\Delta E_e}{E_e} = \frac{10\%}{\sqrt{E_e(\mathrm{GeV})}} \oplus 0.7\%,$$
$$\frac{\Delta E_j}{E_j} = \frac{50\%}{\sqrt{E_j(\mathrm{GeV})}} \oplus 3\%. \tag{58}$$

3. Results

We ran our Monte Carlo for the LHC at 14 TeV center-of-mass energy for the signal process in Fig. 15. We used CTEQ 4M parton distribution functions [26]; and, all results are presented at parton level. α_s is computed at two-loop level. At zero order in the $SU(2)_D$ gauge coupling, the model admits "Z_2-like" topologies. We show the kinematic edge resulting from this topology in Fig. 7. We also include SM the dominant $\bar{t}t$ as well as the irreducible $Z \to \bar{\nu}\nu$ backgrounds. To order α in the $SU(2)_D$ coupling, we have six additional diagrams which generate corrections. For completeness, in appendix B, we list all of the different topologies and plot each correction before interfering the diagram to get Fig. 7. Each diagram listed in the appendix is instructive for the shape and position for each kinematic edge. The kinematic cuts listed in Sec. IVA 2 are taken; the shapes of the distribution are generally preserved under the cuts. The total irreducible background events from $Z \to \bar{\nu}\nu$ and the dilepton $\bar{t}t$ channel for 100 fb^{-1} is

$$B_{Z\to\bar{\nu}\nu} = 98.5 \qquad B_{\bar{t}t} = 56630. \tag{59}$$

Additionally, total signal events (Fig. 8) for 100 fb^{-1}

$$S = 4440, \tag{60}$$

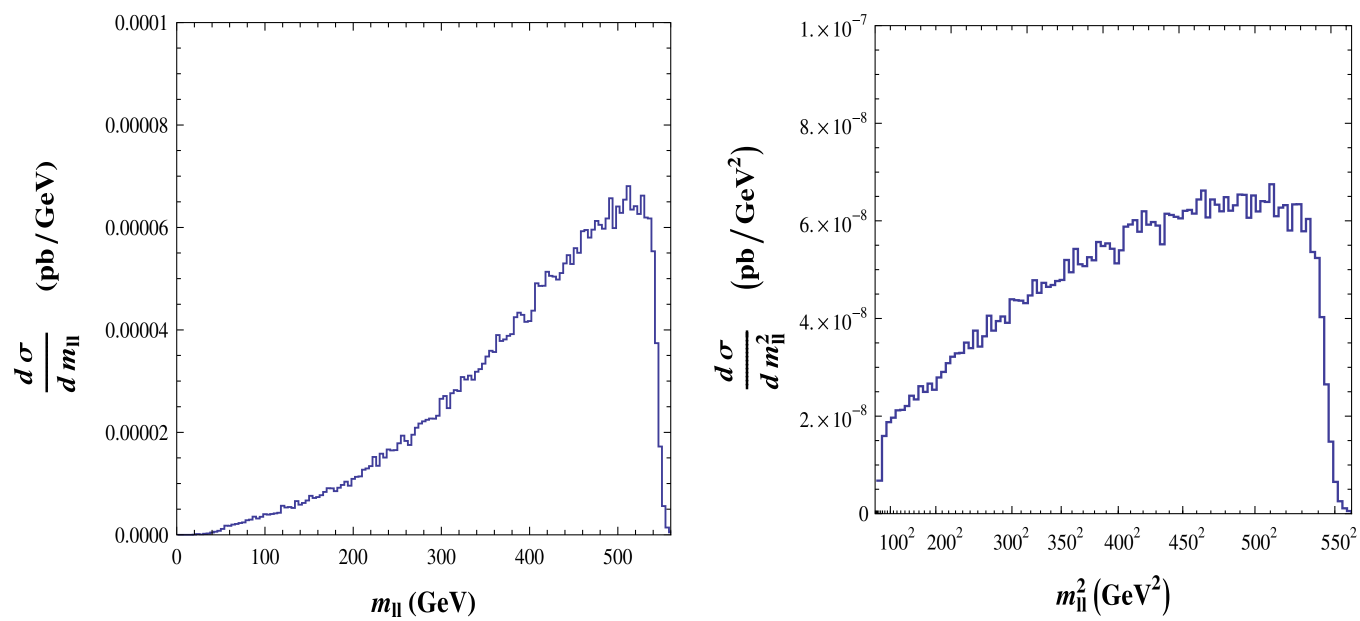

FIG. 7 (color online). Dilepton invariant mass (left panel) and invariant mass squared (right panel) distributions for the topology in Fig. 6. The cuts described in Sec. IVA 2 are applied.

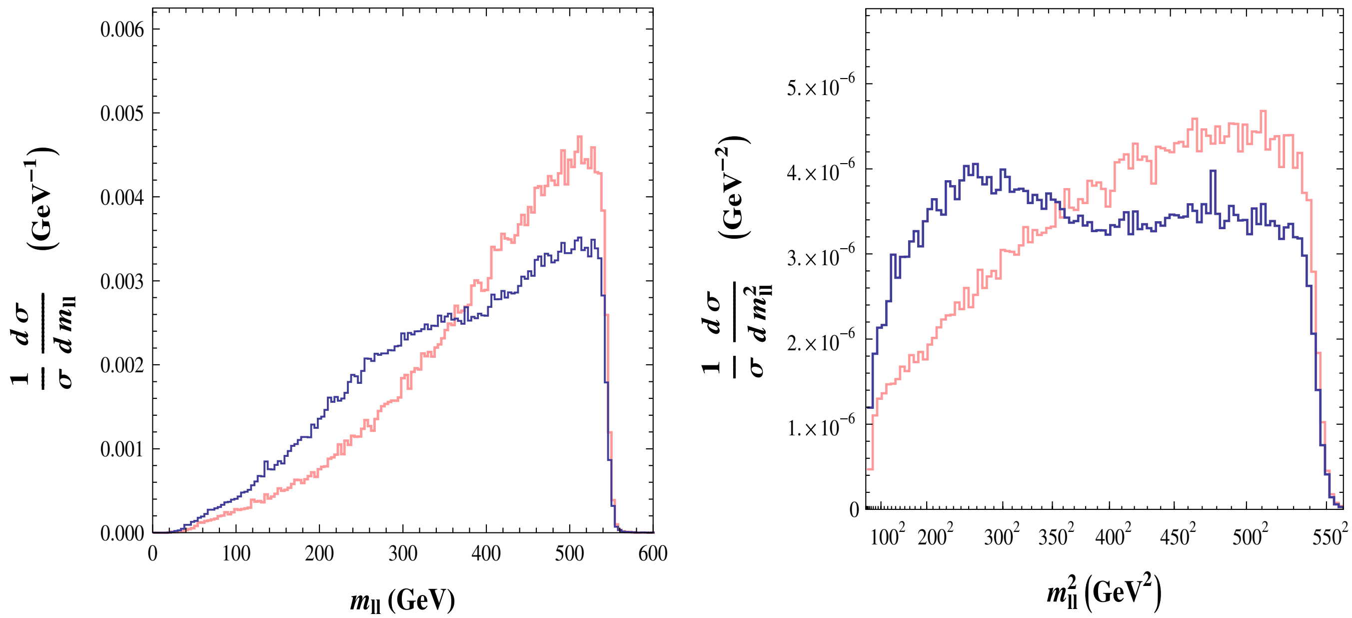

FIG. 8 (color online). Dilepton invariant mass (left panel) and invariant mass squared (right panel) distributions but with the first order corrections from the long-lived gauge bosons. The left panel features the double kinematic edge. The edges are roughly separated by the 100 GeV gauge boson mass. The Z_2-like signal is also plotted for comparison as well as the backgrounds described in the figure above. All of the topologies generated by the long-lived gauge bosons are listed and individually plotted in Appendix B.

which generates the following signal-to-background ratio and statistical significance for signal observability

$$S/B = 0.08 \qquad S/\sqrt{B} = 18.6. \tag{61}$$

B. Warped GUT

We present another very well-motivated Z_3 model: for more details, see the original Refs. [17,18]. This model is based on the framework of a warped extra dimension with the SM fields propagating in it which can address both the Planck-weak and flavor hierarchy problems of the SM [27]. In a grand unified theory (GUT) model within this framework, it was shown that

(i) a viable DM particle can emerge a *spin-off* of suppressing proton decay.

Moreover,

(ii) Z_3 (rather than Z_2) as the symmetry stabilizing DM arises naturally (due to combination of SM color and baryon number quantum numbers).

It turns out that the SM particles resulting from the decay of mother particles in this model are mostly top quarks and W's. We defer an analysis of the reconstruction of these decay chains to future work. Here we simply give a summary of this model and the relevant LHC signals.

1. Basic framework

In this framework, the SM particles are identified as zero-modes of 5D fields, whereas the heavier modes (i.e., nontrivial excitations of the SM particles in the extra dimension) are denoted by Kaluza-Klein or KK particles and constitute the new physics. A few TeV KK mass scale can be consistent with electroweak and flavor precision tests, at the same time avoiding at least a severe fine-tuning of the weak scale [27].

An extension of the SM gauge group in the bulk to GUT gauge group is motivated by precision unification of gauge couplings and explanation of quantization of hypercharge. In more detail, the extra/non-SM 5D gauge bosons (denoted generically by X) do not have zero-modes by, for example, an appropriate choice of boundary conditions. However, these gauge bosons still have KK modes with a *few TeV* mass (i.e., same as SM gauge KK modes), instead of usual mass of $\sim O(10^{15})$ GeV in 4D-like GUTs. The fermions follow a different story as follows. The 5D fermion fields must of course form complete GUT multiplets. Usually, an entire SM generation fits in such a complete multiplet(s), for example, **16** for $SO(10)$ GUT group, i.e., quark-lepton unification is incorporated. However, if we attempt to identify SM fermions of one generation as *zero modes* of a complete 5D GUT multiplet, then it turns out that we will get too fast proton decay via exchange of X between SM quarks and leptons—again, with a few TeV mass.[13]

[13]It turns out that the couplings of X to SM quarks and leptons are suppressed – roughly by powers of SM Yukawa couplings—due to the nature of the profiles in the extra dimension of the various particles, but this effect is not sufficient to allow a few TeV mass for X to be consistent with proton decay.

2. Split fermion multiplets

Fortunately, the breaking of GUT gauge group down to SM gauge group by boundary condition allows "split" fermion multiplets (just like for gauge bosons) as follows. We can choose boundary conditions such that one 5D multiplet (labeled "quark" multiplet) has zero-mode only in its quark component, with the leptonlike component having only KK mode and vice versa for another multiplet (labeled "lepton" multiplet'). Thus SM quarks and leptons originate from *different* 5D multiplets, avoiding exchange of X gauge bosons between SM quarks and leptons since such exchange can only couple fermions (whether zero or KK-modes) within the *same* 5D fermion multiplet. In spite of this "loss" of quark-lepton unification, the explanation of hypercharge quantization is still maintained since SM quark must still be *part* of a complete GUT multiplet. In fact, such splitting of fermion multiplets results in precision unification of couplings in the model where the GUT group is broken down to the SM on the Planck brane [28]. The reason for the modification relative to the running in the SM (and hence the improvement in the unification) is the different profiles for quarks and leptons, especially within the third generation.

3. Additional symmetry for proton stability

It turns out that to maintain this suppression of proton decay at higher orders, we have to impose an extra symmetry, for example, a gauged $U(1)_B$ [commuting with the GUT group] in the bulk as follows. The *entire* quark multiplet is assigned $B = 1/3$ (i.e., that of the zero-mode contained in this multiplet). Thus leptonlike states from this multiplet are "exotic" in the sense that they have $B = 1/3$. Similarly, the entire lepton multiplet is assigned $B = 0$, giving exotic quarklike states (i.e., with $B = 0$). X's are also exotic since they are colored, but have $B = 0$. The exoticness is especially striking since these states cannot decay into purely SM: explicitly, they are charged under a symmetry

$$\Phi \longrightarrow e^{2\pi i((\alpha-\bar{\alpha}/3)-B)}\Phi \tag{62}$$

(where α, $\bar{\alpha}$ are the number of color, anticolor indices on a field Φ), under which SM is neutral.[14] Thus the lightest Z_3-charged particle (dubbed "LZP") is stable (others Z_3-charged particles produced in colliders or in the early, hot universe decay into it) and a potential DM candidate, depending on its couplings.

4. Who's the LZP/DM?

In the model with GUT group broken to the SM on the Planck brane which was the focus in Refs. [17,18], it turns out that, due to profile of t_R (in turn, based on heaviness of top quark and constraint from shift in $Zb\bar{b}$ coupling), its exotic GUT partners are lighter that typical KK scale (say, mass of gauge KK modes). Thus, it is very likely that LZP resides in this multiplet. In particular, if the GUT group is $SO(10)$, then there is a GUT partner of t_R with quantum numbers of right-handed (RH) neutrino, but with $B = 1/3$ (denoted by ν'_R and its LH Dirac partner, denoted by $\hat{\nu}'_R$). It has been shown that if this ν' is the LZP,[15] then it is a good DM candidate, in the sense that, in some regions of parameter space, it has the correct relic density upon thermal freeze-out in the early universe: see Fig. 5 of Ref. [18] and Figs. 3 and 4 of Ref. [29] (the latter reference studies a modified version of the model outlined here) and related discussion. Similarly, the constraints from direct detection of DM can be satisfied: see Fig. 7 of Ref. [18] and Fig. 3 of Ref. [29] and related discussion. Other GUT partners of t_R are then heavier than ν', but they can still be lighter than SM gauge KK modes. And, GUT partners of *other* SM particles, including X-type gauge bosons, are as heavy as SM gauge KK modes.

5. DM partner at the LHC

As usual, in order to test this idea at colliders, we consider producing the (other than LZP) Z_3-charged particles at colliders (of course, these must be produce in pairs) and observe their decays into SM particles and LZP. Since colored and lightest such particles will have largest cross-section at the LHC, a good candidate for such a study is the GUT partner of t_R with $(t, b)_L$ quantum numbers, denoted by (t'_L, b'_L) [and its conjugate by $(\hat{t}'_L, \hat{b}'_L)$].[16] The two states t' and b' are degenerate before EWSB, but will be split afterward.

We focus here on b' due to the interesting features in its decay channels as shown in Fig. 9. X_s, the $SU(2)_L$ doublet X, Y and another $SU(2)_L$ doublet X', Y' are beyond SM gauge bosons of $SO(10)$, with electric charges $2/3$, $4/3$, and $1/3$, and $2/3$ and $1/3$, respectively.[17] First of all, the 1st decay chain of b' into two DM (ν'_R) and tW does have the topology needed to give a cusp in the invariant mass of SM/visible particles (of course assuming on-shell inter-

[14] In more detail, $U(1)_B$ has to be broken to avoid zero-mode gauge boson. We break it on the Planck brane so that 4-fermion operators giving proton decay [i.e., violating $U(1)_B$] can only arise on the Planck brane where they are adequately suppressed. However, $U(1)_B$ still cannot be broken arbitrarily, i.e., a subgroup of $U(1)_B$ must still be preserved in order to forbid (mass) mixing of lepton and quark multiplets on the Planck brane which will lead to rapid proton decay—for example, we require that the scalar vev which breaks $U(1)_B$ has $B =$ integer in which case the above Z_3 symmetry is still preserved, even if $U(1)_B$ is broken.

[15] At leading order, all the GUT partners of t_R are degenerate, but higher-order effects can split them.

[16] Recall that the $(t, b)_L$ and *conjugate* of t_R are contained in the same representation, namely, **16** of $SO(10)$ so that the (t'_L, b'_L) states with $B = -1/3$ are indeed exotic.

[17] Note that only the 1st decay channel is shown in Fig. 10 of Ref. [18].

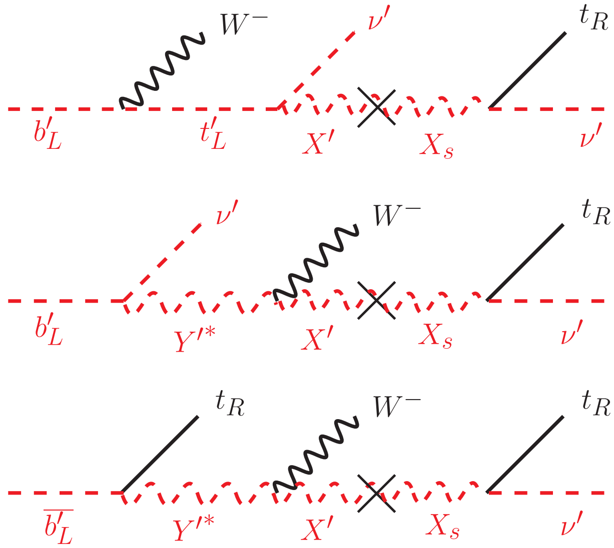

FIG. 9 (color online). Different possible decay chains for b' in the scenario of [18]. Note the appearance of two DM states in two of the possible decay chains, whereas only one DM particle comes out of the third possibility.

mediate particles; see comment below). Second, the 2nd process above involves the same final state, but with a different topology and thus is relevant for obtaining multiple edges (again, with on-shell intermediate particles), even with two DM in final state. However, it is clear that the intermediate particles (X-type gauge bosons) in the above processes are actually *off*-shell so that these features are not so useful for us here. Finally, while there does not seem to be a decay of b' into tW and one DM which would be relevant for obtaining double edge with off-shell intermediate particles (when combined with the 1st and 2nd processes above with two DM), there is a decay to tWW and one DM (i.e., with an "extra" W) as in the 3rd process above which might play this role. Thus, decay of b' will exhibit a double edge due to presence of one DM and two DM in final state [along the lines of the discussion of Eq. (2.1.2)]: $M_{b'} - 2M_{\nu'} - m_t - m_W$ (for 1st and 2nd processes) and $M_{b'} - M_{\nu'} - 2m_t - m_W$ (for 3rd process).

Note that, in a nonminimal model, for example, if $SO(10)$ is broken on the TeV brane instead of the Planck brane, the X's bosons might be lighter so that the intermediate particles in decay chains similar to those above might be on shell. However, then we might as well study production of the lighter X's (instead of the exotic fermions) which are also colored and which will decay into LZP via *off*-shell GUT partners of SM fermions.

V. CONCLUSIONS AND OUTLOOK

Many extensions of the SM contain stable WIMPs which can be viable DM candidates. Most of these models stabilize the DM with a parity (Z_2) symmetry. However, in the spirit that all fundamental particles in nature are defined by how they transform under different symmetries, these models actually correspond to one type of candidate! On the other hand, any continuous or discrete global symmetry can be adopted for DM stabilization; and, DM candidates stabilized by a parity symmetry and, e.g., a Z_3 symmetry are different.

This possibility of other than Z_2 symmetries stabilizing DM is more than just of academic interest; the nature of the stabilization symmetry has important implications on collider searches for DM. At colliders other particles (heavier than DM) which are charged under the same symmetry

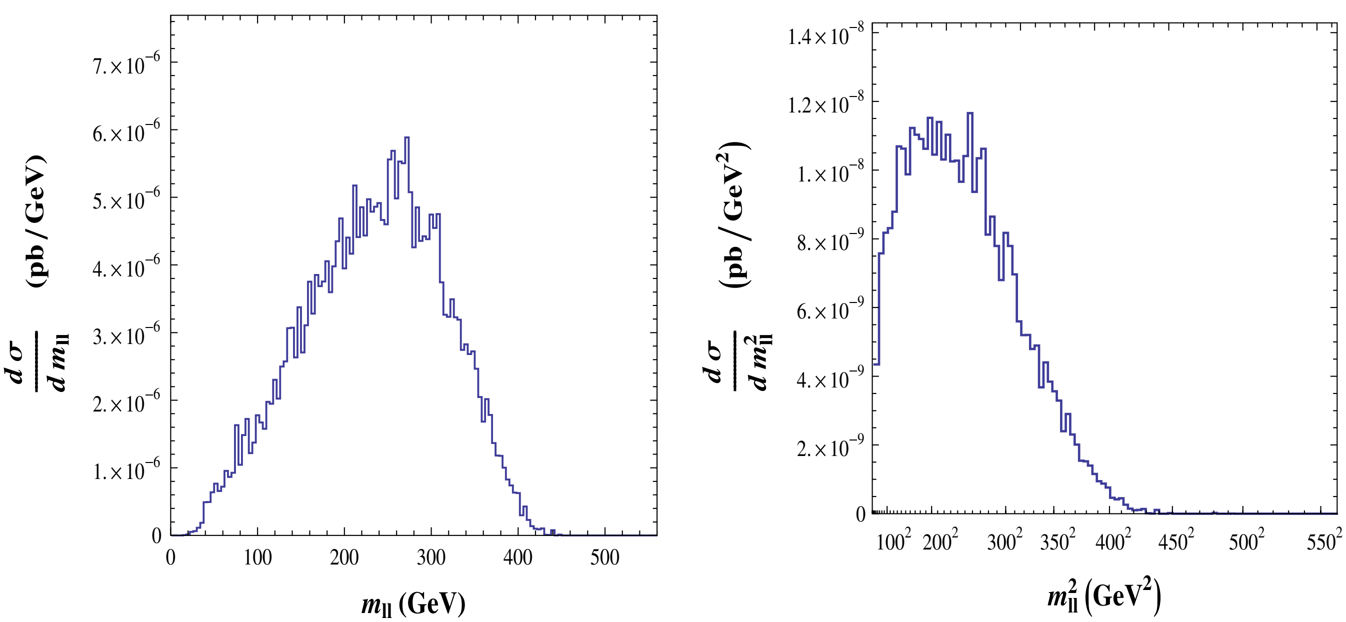

FIG. 10 (color online). The plots corresponding to the topology of Eq. (B1).

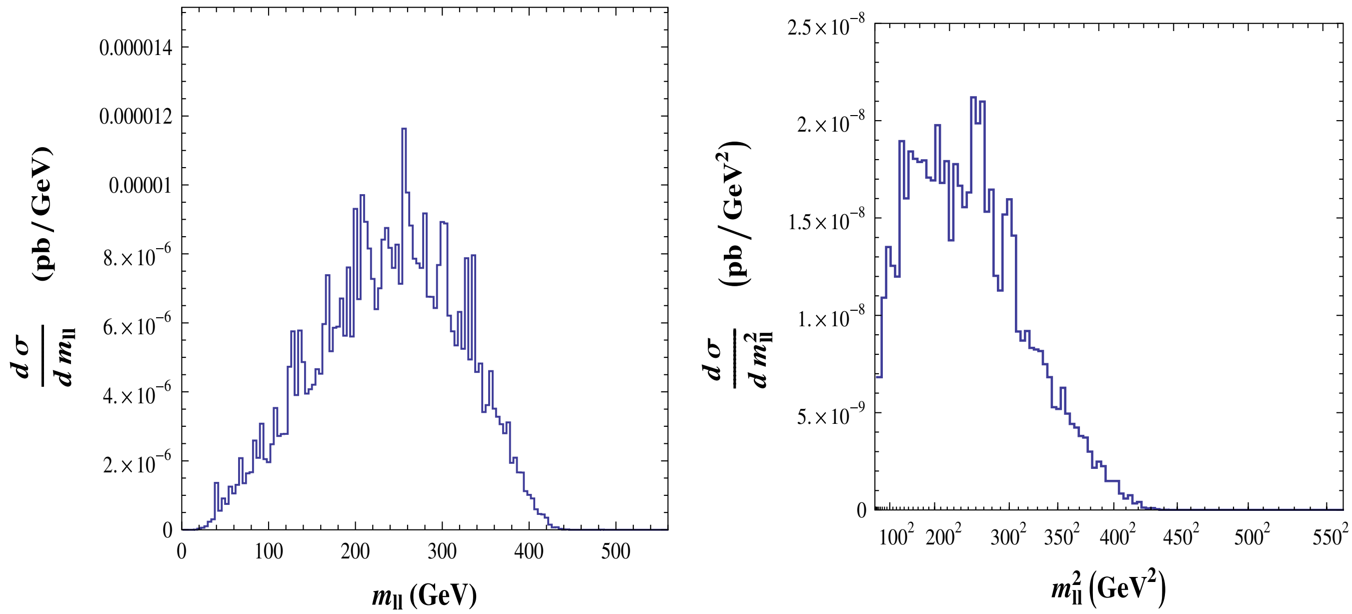

FIG. 11 (color online). The plots corresponding to the topology of Eq. (B2).

which stabilizes the DM candidate(s) can be produced, decaying into DM and SM particles. Such events will generate decay topologies and modes that are determined, in part, by the stabilization symmetry. Thus the analysis of such "missing energy" signals will present a hint not only for the existence of the DM but also the nature of its stabilization symmetry.

For example, the decay of a *single* such mother particle can contain one or two DM in the case of a Z_3 symmetry, but only one in the case of Z_2 symmetry. We showed that in many cases simple kinematic observables, such as invariant mass distributions of the visible particles of such decay chain, could then characterize the stabilizing symmetry. Specifically, when a mother particle decay via off-shell intermediate states into the same visible particles along with one and two DM (for the case of Z_3 symmetry), it may be possible to observe a *double edge* in the distribution of these visible particles (vs. single edge for Z_2 symmetry). In fact, the difference between the location of the edges will be a direct measure of the mass of the dark matter particle for Z_3 models. On the other hand, when the intermediate particles are on-shell, we also pointed out the possibility of

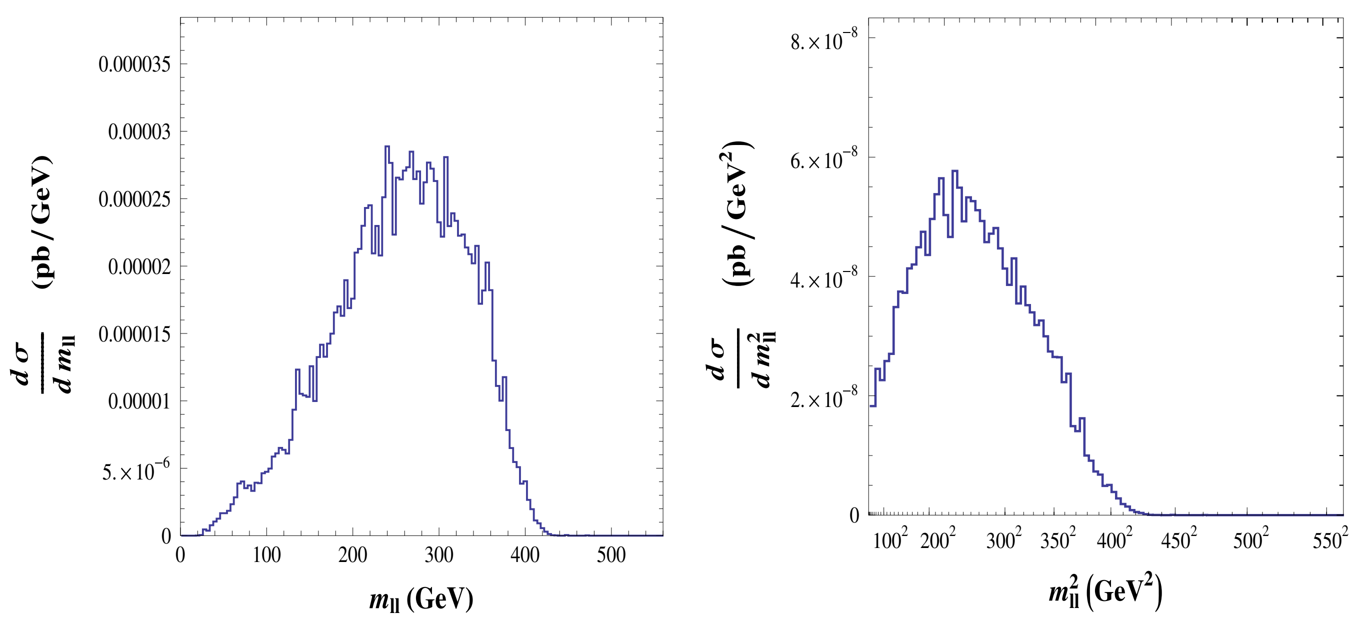

FIG. 12 (color online). The plots corresponding to the topology of Eq. (B3).

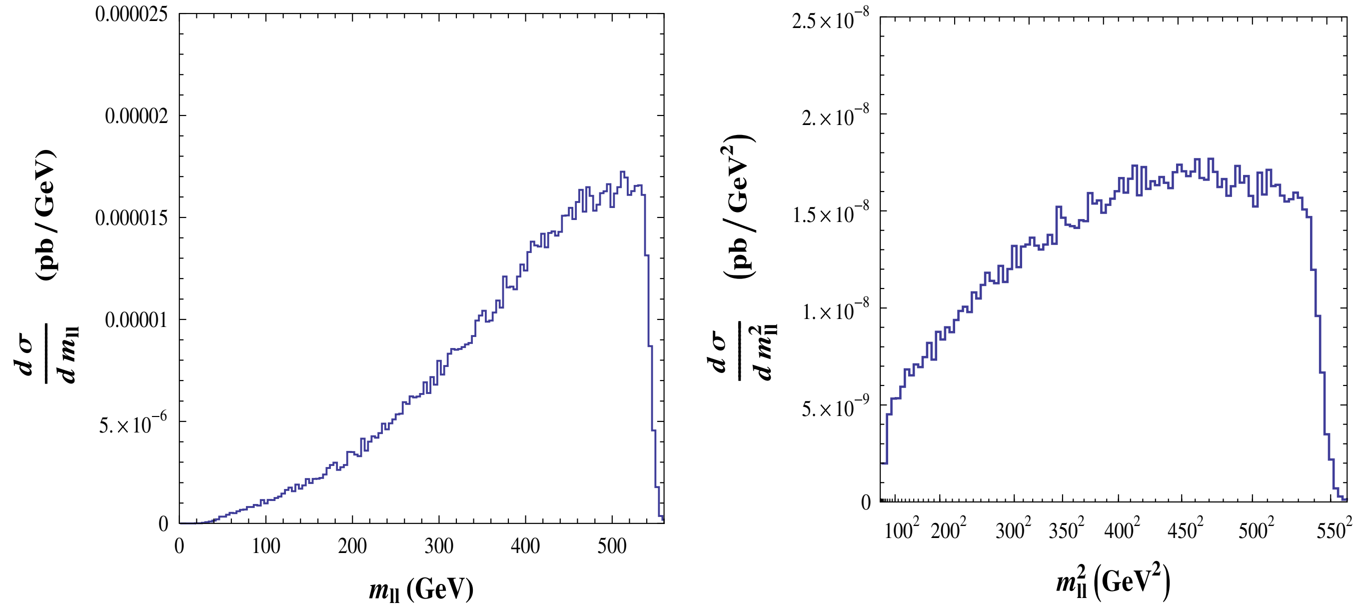

FIG. 13 (color online). The plots corresponding to the topology of Eq. (B4).

a very distinctive feature appearing in the invariant mass distribution of *two* visible particles in the case of Z_3 symmetry: a cusp dividing the distribution into two regions. This happens when two DM particles emerge from the same chain, with one of these DM particles being situated in between the two SM particles.

A. Signal fakes

We point out that models with parity stabilized dark matter can naively fake *double kinematic edges* and *cusps*. An example of a faked cusp comes from a decay chain with on-shell intermediate particles and involving a SM neutrino(s) in the final state. If a neutrino is emitted between the two other, visible SM particles, then we obtain the new topology considered above so that the invariant mass distribution of the two visible SM particles can give a cusp. As another example, a double kinematic edge also comes from two different mother particles charged under Z_2 which could be produced in separate events [30], but with same visible decay products[18] Also, in this paper, we considered decays of mother particle into DM and SM particles occurring inside the detector. However, a long-lived, parity odd particle in a Z_2 model that decays outside of the detector can fake our Z_3 signal. For example, a single mother can decay into such a particle and SM particles. The same mother can also decay to the same SM final state and the DM. A combination of these two decay chains can generate a double edge. A closely related scenario is that there are actually two (absolutely) stable DM particles in a Z_2 model [31], again giving double edges from two decay chains (along the lines just mentioned). Finally, if there are *more than* two SM particles involved in the decay of a single mother, the analysis of the cusp in the invariant mass distribution will be more complicated, but nevertheless we expect that in general the same type of arguments made here should be able to be implemented in this case. As an example, a possible *pseudo*-faking situation will arise when three visible particles are emitted in a decay cascade in the Z_2 case. However, we mentioned how this type of faking can be resolved by considering all possible pair invariant masses.

B. Future considerations

Of course, in any given event, there will be two such mother particles present[19] (three mothers is a possibility in Z_3 case, but it is phase-space suppressed). The assumption of a Z_2 symmetry thus points to an eventual emergence of two invisible particles for every new physics event in the collider. On the other hand, models where dark matter is stabilized with, e.g. Z_3 symmetry, can have two, three, or four dark matter candidates in an event. In an ongoing work, we construct a variant of the m_{T2} and m_{TX} variables [4] to use the information on both decay chains in the full

[18]Note that, assuming pair production, multiple mothers in Z_2 cannot fake different edges in two distributions that we discussed in Sec. II B.

[19]However, studying the decay of only one mother (as we have mostly done in this paper) is still relevant, for example, if this decay involves a "clean" (SM) final state (vs. a dirtier one from the other mother). Of course, we also need to determine *experimentally* which SM particles in the event came from this decay chain, which is possible, for example, if this mother is boosted in the laboratory frame so that the decay products are roughly collimated.

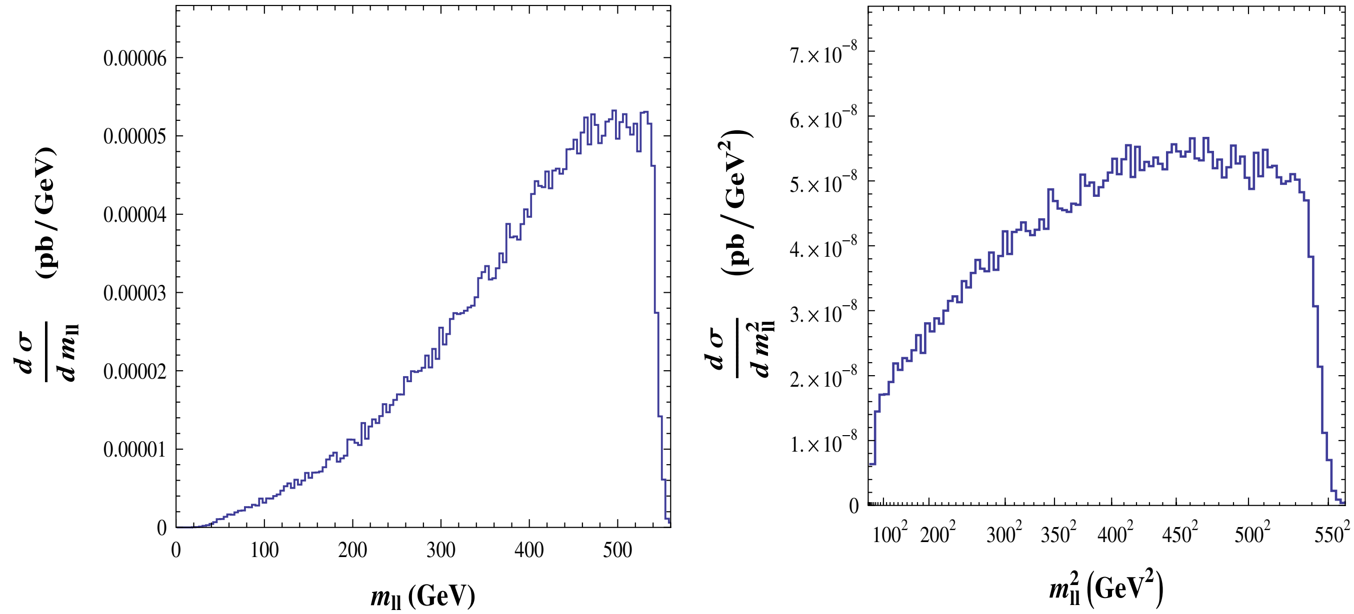

FIG. 14 (color online). The plots corresponding to the topology of Eq. (B5).

event. The goals of such techniques are to establish that the DM is stabilized by a Z_3 symmetry in other situations which were not discussed here, e.g., when a cusplike topology is absent, and to better eliminate the fakes of Z_3 signal by Z_2 models. We also are studying other techniques to eliminate the fakes described above.

In all, we emphasize that parity symmetries are not necessarily the only way to stabilize the DM and we showed (via a few example cases) that models with other stabilization symmetries generally have testable consequences at the LHC, i.e., can potentially be distinguished from the parity case. The reader should regard this work as a first step into a more complete study of *beyond* Z_2 stabilized dark matter scenarios.

ACKNOWLEDGMENTS

We would like to thank I. Hinchliffe, A. Katz, G. Servant, M. D. Shapiro, R. Sundrum and B. Tweedie for valuable discussions. K. A. was supported in part by NSF Grant No. PHY-0652363.

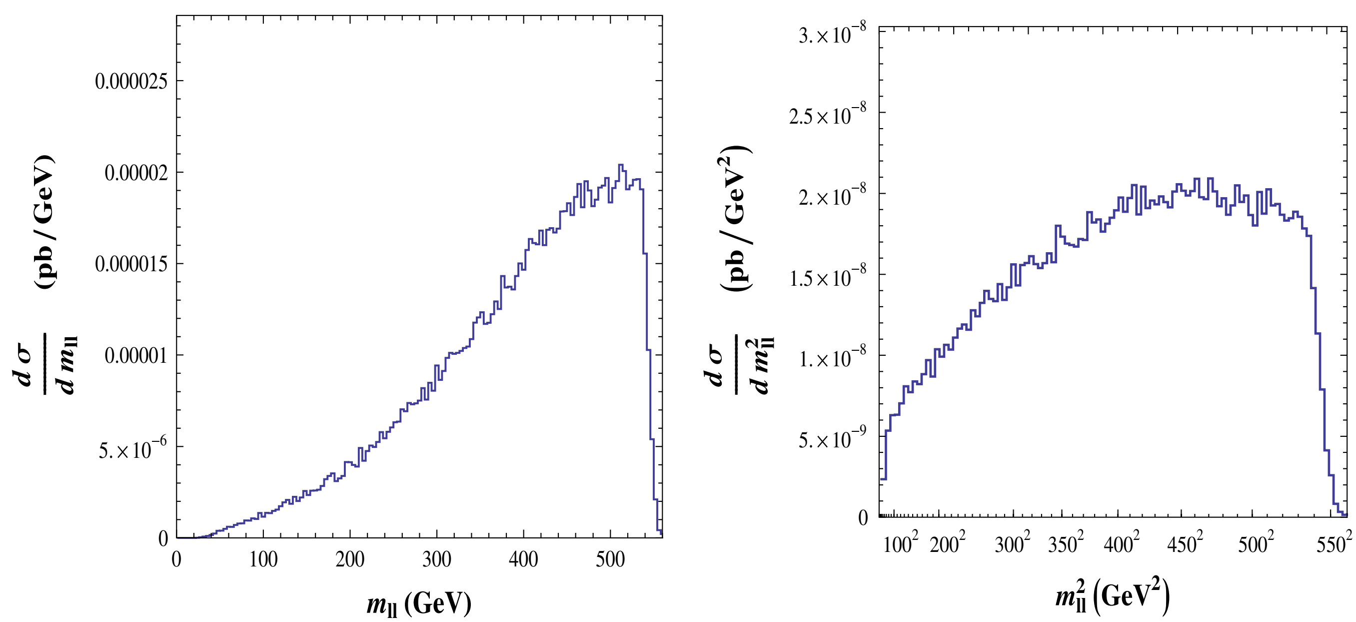

FIG. 15 (color online). The plots corresponding to the topology of Eq. (B5).

APPENDIX A: THE DISTRIBUTION FOR THE NEW TOPOLOGY

Most of the intermediate steps in the derivation of the cusp in Eq. (28) are similar to the analysis in Ref. [21] of the reaction in Eq. (21), except for the fact that a DM (i.e., massive) particle is situated in between two SM particles in the new topology [See Eq. (24)]. Based on the algebra and the notations found in Ref. [21], we will derive a few useful relations.

Basically, the invariant mass formed by the two SM particles in this topology is given by

$$m_{ca}^2 = (p_c + p_a)^2 = 2E_c E_a(1 - \cos\theta_{ca}) \tag{A1}$$

where θ_{ca} is the opening angle between two visible particles. Note that this relation is always valid in any frame so that we can rewrite the above relation as

$$m_{ca}^2 = 2E_c^{(B)} E_a^{(B)}(1 - \cos\theta_{ca}^{(B)}). \tag{A2}$$

Here and henceforth the (particle) superscripts on θ's (in this case B) imply that those angles are measured in the rest frame of the corresponding particle. Using energy-momentum conservation, we can easily obtain the energies for a, DM, and c, which are measured in the rest frame of particle B.

$$E_a^{(B)} = \frac{m_B^2 - m_A^2}{2m_B} \tag{A3}$$

$$E_{\mathrm{DM}}^{(B)} = \frac{m_C^2 - m_B^2 - m_{\mathrm{DM}}^2}{2m_B} \tag{A4}$$

$$E_c^{(B)} = \frac{(m_D^2 - m_C^2)m_B}{m_B^2 + m_C^2 - m_{\mathrm{DM}}^2 - \lambda^{1/2}(m_C^2, m_B^2, m_{\mathrm{DM}}^2)\cos\theta_{c\mathrm{DM}}^{(B)}} \tag{A5}$$

Inserting these relations into Eq. (A2), we obtain

$$m_{ca}^2 = 2 \cdot \frac{(m_D^2 - m_C^2)m_B}{m_B^2 + m_C^2 - m_{\mathrm{DM}}^2 - \lambda^{1/2}(m_C^2, m_B^2, m_{\mathrm{DM}}^2)\cos\theta_{c\mathrm{DM}}^{(B)}} \cdot \frac{m_B^2 - m_A^2}{2m_B}(1 - \cos\theta_{ca}^{(B)}). \tag{A6}$$

We easily see that the maximum of m_{ca}^2 occurs when $\cos\theta_{c\mathrm{DM}}^{(B)} = 1$ and $\cos\theta_{ca}^{(B)} = -1$. We want to express the invariant mass m_{ca} in terms of variables which have flat distributions: this is the case for $\cos\theta_{ca}^{(B)}$, but not for $\cos\theta_{c\mathrm{DM}}^{(B)}$. So, we need to express $\cos\theta_{c\mathrm{DM}}^{(B)}$ in terms of $\cos\theta_{c\mathrm{DM}}^{(C)}$ (i.e., the same angle in the rest frame of particle C) for which the distribution is also flat. This relation can be found by calculating $m_{c\mathrm{DM}}^2$ in the rest frames of particle C and B:

$$m_{c\mathrm{DM}}^2 = m_{\mathrm{DM}}^2 + 2E_c^{(C)}E_{\mathrm{DM}}^{(C)} - 2E_c^{(C)}\sqrt{(E_{\mathrm{DM}}^{(C)})^2 - m_{\mathrm{DM}}^2}\cos\theta_{c\mathrm{DM}}^{(C)} \tag{A7}$$

$$= m_{\mathrm{DM}}^2 + 2E_c^{(B)}E_{\mathrm{DM}}^{(B)} - 2E_c^{(B)}\sqrt{(E_{\mathrm{DM}}^{(B)})^2 - m_{\mathrm{DM}}^2}\cos\theta_{c\mathrm{DM}}^{(B)} \tag{A8}$$

Again, the energy-momentum conservation in the rest frame of C gives the following relations:

$$E_{\mathrm{DM}}^{(C)} = \frac{m_C^2 - m_B^2 + m_{\mathrm{DM}}^2}{2m_C} \tag{A9}$$

$$E_c^{(C)} = \frac{m_D^2 - m_C^2}{2m_C} \tag{A10}$$

Substitution of E_{DM} and E_c in the rest frame of C and B into Eq. (A7) and (A8) gives the relation between $\cos\theta_{c\mathrm{DM}}^{(B)}$ and $\cos\theta_{c\mathrm{DM}}^{(C)}$:

$$\frac{2m_B^2}{m_C^2 + m_B^2 - m_{\mathrm{DM}}^2 - \lambda^{1/2}(m_C^2, m_B^2, m_{\mathrm{DM}}^2)\cos\theta_{c\mathrm{DM}}^{(B)}} = \left(1 - \frac{m_C^2 - m_B^2 + m_{\mathrm{DM}}^2 - \lambda^{1/2}(m_C^2, m_B^2, m_{\mathrm{DM}}^2)\cos\theta_{c\mathrm{DM}}^{(C)}}{2m_C^2}\right) \tag{A11}$$

Next, we introduce the variables u and v:

$$u \equiv \frac{1 - \cos\theta_{c\mathrm{DM}}^{(C)}}{2}, \qquad v \equiv \frac{1 - \cos\theta_{ca}^{(B)}}{2} \tag{A12}$$

and using Eq. (A11), we express m_{ca}^2 in terms of u and v:

$$m_{ca}^2 = (m_{ca}^{\max})^2(1 - \alpha u)v \tag{A13}$$

where

$$(m_{ca}^{\max})^2 = \frac{2(m_D^2 - m_C^2)(m_B^2 - m_A^2)}{m_B^2 + m_C^2 - m_{\mathrm{DM}}^2 - \lambda^{1/2}(m_C^2, m_B^2, m_{\mathrm{DM}}^2)}. \tag{A14}$$

Note that the differential distributions for u and v ($0 \le u$, $v \le 1$) are also flat:

$$\frac{1}{\Gamma}\frac{\partial^2\Gamma}{\partial u \partial v} = \theta(u)\theta(1 - u)\theta(v)\theta(1 - v) \tag{A15}$$

where $\theta(x)$ is the usual step function. Replacing u and v by u and m_{ca}^2 by using Eq. (A13) gives the differential distribution

$$\frac{1}{\Gamma}\frac{\partial^2\Gamma}{\partial u \partial m_{ca}^2} = \hat{\theta}\left(\frac{m_{ca}^2}{(m_{ca}^{\max})^2(1 - \alpha u)}\right)\frac{\hat{\theta}(u)}{(m_{ca}^{\max})^2(1 - \alpha u)} \tag{A16}$$

where a "top-hat" function $\hat{\theta}(x) \equiv \theta(x)\theta(1 - x)$. The next step is to integrate over u to find the distribution in m_{ca}^2:

$$\frac{1}{\Gamma}\frac{\partial^2\Gamma}{\partial m_{ca}^2} = \int_{-\infty}^{\infty}\frac{1}{\Gamma}\frac{\partial^2\Gamma}{\partial u \partial m_{ca}^2}du = \int_0^1 \hat{\theta}\left(\frac{m_{ca}^2}{(m_{ca}^{\max})^2(1-\alpha u)}\right)\frac{1}{(m_{ca}^{\max})^2(1-\alpha u)}du = \int_0^{u_{\max}}\frac{1}{(m_{ca}^{\max})^2(1-\alpha u)}du \tag{A17}$$

for $0 \le m_{ca} \le m_{ca}^{\max}$, where

$$u_{\max} = \mathrm{Max}\left(1, \frac{1}{\alpha}\left[1 - \frac{m_{ca}^2}{(m_{ca}^{\max})^2}\right]\right). \tag{A18}$$

Now the above integral is easy to evaluate, and we finally obtain the distribution which was given earlier in Eq. (28):

$$\frac{1}{\Gamma}\frac{\partial^2\Gamma}{\partial m_{ca}^2} = \begin{cases} \frac{1}{(m_{ca}^{\max})^2\alpha}\ln\frac{m_C^2}{m_B^2} & \text{for } 0 < m_{ca} < \sqrt{1-\alpha}\, m_{ca}^{\max} \\ \frac{1}{(m_{ca}^{\max})^2\alpha}\ln\frac{(m_{ca}^{\max})^2}{m_{ca}^2} & \text{for } \sqrt{1-\alpha}\, m_{ca}^{\max} < m_{ca} < m_{ca}^{\max}. \end{cases} \tag{A19}$$

APPENDIX B: SIGNAL TOPOLOGIES FROM SEC. IVA 1

In addition to the decay chain in Fig. 6 for the model presented in Sec. IVA, there are additional corrections by the long-lived $SU(2)_D$ gauge bosons. The masses are listed in Eq. (49). As described above, the virtual particles in the decay chain go slightly off-shell when emitting the new gauge boson; however, because there are three of them, the additional multiplicity factor helps to ameliorate this suppression. In this appendix for each topology, we plot the invariant mass distributions with the cuts in Sec. IVA 2 (see Figs. 10–15).

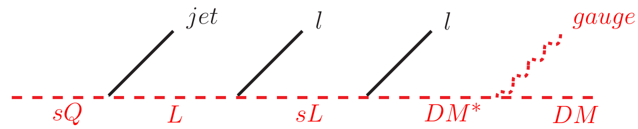

(B1)

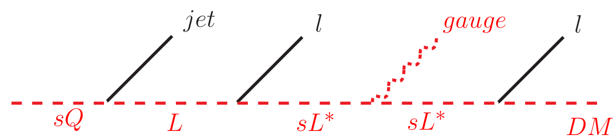

(B2)

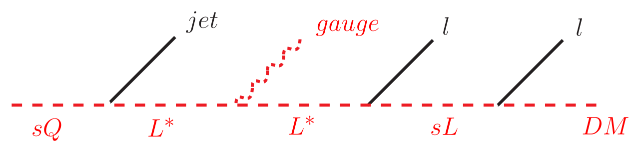

(B3)

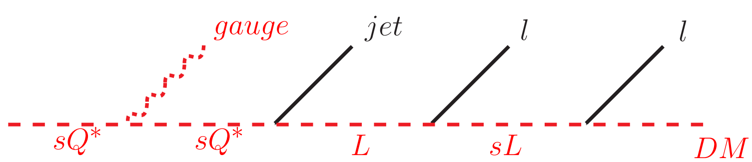

(B4)

Equations (B1)–(B4): Order α corrections by the $SU(2)_D$ gauge bosons to the decay chain in Fig. 6. See the model in Sec. IVA.

(B5)

Equation (B5): Order α corrections by the $SU(2)_D$ gauge bosons to the decay chain in Fig. 6. See the model in Sec. IVA.

[1] See, for example, G. Bertone, D. Hooper, and J. Silk, Phys. Rep. **405**, 279 (2005).

[2] G. Hinshaw *et al.* (WMAP Collaboration), Astrophys. J. Suppl. Ser. **180**, 225 (2009).

[3] E. W. Kolb and M. S. Turner, Front. Phys. **69**, 1 (1990).

[4] C. G. Lester and D. J. Summers, Phys. Lett. B **463**, 99 (1999); A. J. Barr, C. G. Lester, M. A. Parker, B. C. Allanach, and P. Richardson, J. High Energy Phys. 03 (2003) 045; A. Barr, C. Lester, and P. Stephens, J. Phys. G **29**, 2343 (2003); W. S. Cho, K. Choi, Y. G. Kim, and C. B. Park, Phys. Rev. Lett. **100**, 171801 (2008); B. Gripaios, J. High Energy Phys. 02 (2008) 053; A. J. Barr, B. Gripaios,

and C. G. Lester, J. High Energy Phys. 02 (2008) 014; W. S. Cho, K. Choi, Y. G. Kim, and C. B. Park, J. High Energy Phys. 02 (2008) 035.

[5] H. C. Cheng, D. Engelhardt, J. F. Gunion, Z. Han, and B. McElrath, Phys. Rev. Lett. **100**, 252001 (2008); H. C. Cheng, J. F. Gunion, Z. Han, and B. McElrath, Phys. Rev. D **80**, 035020 (2009).

[6] K. T. Matchev, F. Moortgat, L. Pape, and M. Park, J. High Energy Phys. 08 (2009) 104; P. Konar, K. Kong, K. T. Matchev, and M. Park, J. High Energy Phys. 04 (2010) 086.

[7] T. Han, I. W. Kim, and J. Song, arXiv:0906.5009.

[8] G. Jungman, M. Kamionkowski, and K. Griest, Phys. Rep. **267**, 195 (1996).

[9] H. S. Lee, Phys. Lett. B **663**, 255 (2008).

[10] H. C. Cheng and I. Low, J. High Energy Phys. 09 (2003) 051; 08 (2004) 061.

[11] G. Servant and T. M. P. Tait, Nucl. Phys. **B650**, 391 (2003); H. C. Cheng, J. L. Feng, and K. T. Matchev, Phys. Rev. Lett. **89**, 211301 (2002).

[12] K. Agashe, A. Falkowski, I. Low, and G. Servant, J. High Energy Phys. 04 (2008) 027.

[13] The ATLAS Collaboration, Report No. CERN-LHCC-99-015.

[14] The CMS Collaboration, J. Phys. G **34**, 995 (2007).

[15] D. G. E. Walker, arXiv:0907.3146.

[16] D. G. E. Walker, arXiv:0907.3142.

[17] K. Agashe and G. Servant, Phys. Rev. Lett. **93**, 231805 (2004).

[18] K. Agashe and G. Servant, J. Cosmol. Astropart. Phys. 02 (2005) 002.

[19] E. Ma, Phys. Lett. B **662**, 49 (2008).

[20] E. Byckling and K. Kajantie, *Particle Kinematics* (John Wiley and Sons, New York, 1973).

[21] D. J. Miller, P. Osland, and A. R. Raklev, J. High Energy Phys. 03 (2006) 034.

[22] S. Kraml and A. R. Raklev, Phys. Rev. D **73**, 075002 (2006).

[23] L. T. Wang and I. Yavin, J. High Energy Phys. 04 (2007) 032.

[24] J. Alwall *et al.*, J. High Energy Phys. 09 (2007) 028.

[25] C. Amsler *et al.* (Particle Data Group), Phys. Lett. B **667**, 1 (2008).

[26] H. L. Lai *et al.*, Phys. Rev. D **55**, 1280 (1997).

[27] For a review and the original references, see H. Davoudiasl, S. Gopalakrishna, E. Ponton, and J. Santiago, arXiv:0908.1968.

[28] K. Agashe, R. Contino, and R. Sundrum, Phys. Rev. Lett. **95**, 171804 (2005).

[29] K. Agashe, K. Blum, S. J. Lee, and G. Perez, Phys. Rev. D **81**, 075012 (2010).

[30] For a supersymmetric example see, H. Baer, A. Mustafayev, E. K. Park, and X. Tata, J. High Energy Phys. 05 (2008) 058.

[31] For some recent studies, see, for example, K. M. Zurek, Phys. Rev. D **79**, 115002 (2009); F. Chen, J. M. Cline, and A. R. Frey, Phys. Rev. D **80**, 083516 (2009); D. Feldman, Z. Liu, P. Nath, and G. Peim, Phys. Rev. D **81**, 095017 (2010); M. Cirelli and J. M. Cline, Phys. Rev. D **82**, 023503 (2010).